

A Monolithic Active Pixel Sensor
Detector for the sPHENIX
Experiment

2 **A Monolithic-Active-Pixel-Sensor-based Vertex Detector (MVTX) for the**
3 **sPHENIX Experiment at RHIC**

4 A proposal submitted to the DOE Office of Science
5 February 3, 2017

6 *DOE Office of Science Program Manager: Dr. Jehanne Gillo*

Proposing Organization: Los Alamos National Laboratory

Collaborating Institutions: Lawrence Berkeley National Laboratory
Massachusetts Institute of Technology
Brookhaven National Laboratory
Univ. of California at Berkeley
Univ. of California at Los Angeles
Univ. of California at Riverside
Central China Normal University *
Univ. of Colorado
Florida State University
Georgia State University
Iowa State University
New Mexico State University
Univ. of New Mexico
Univ. of Science and Technology of China *
Purdue University *
Univ. of Texas at Austin
Yonsei University
RIKEN/RBRC

Principal Investigator: Ming X. Liu

Phone: 505-412-7396
Email: mliu@lanl.gov

Co-Investigators: Grazyna Odyniec (LBNL) and Robert Redwine (MIT)

Requested Funding: \$4.9M, FY18-FY21

7 * **Note:** Expressed interest to join the sPHENIX Collaboration.

8 **Table of Contents**

9 **Abstract** **iii**

10 **Proposal Narrative** **1**

11 **1 Executive Summary** **1**

12 **2 Physics Goals** **2**

13 2.1 *B*-meson physics at low p_T 2

14 2.2 *b*-jet physics at intermediate p_T 3

15 **3 Detector Requirements** **4**

16 3.1 Physics-driven detector requirements for MVTX 4

17 **4 Technology Choices and Detector Layout** **5**

18 4.1 Design goals and technology choice 5

19 4.2 Detector layout 6

20 **5 Physics Performance** **8**

21 5.1 *b*-jet tagging 9

22 5.2 *B*-meson tagging 12

23 5.3 Event pileup effects 14

24 **6 Technical Scope and Deliverables** **15**

25 6.1 MAPS chips and stave production 15

26 6.2 Readout integration and testing 15

27 6.3 Mechanical carbon structures 16

28 6.3.1 General requirements 16

29 6.3.2 Detector support structure 17

30 6.3.3 Service support structure 17

31 6.4 Mechanical integration 18

32 6.5 Power System 19

33 6.5.1 Power system requirements 19

34 6.5.2 Power system architecture 20

35 6.6 MAPS stave assembly and testing at CERN 21

36 6.7 Detector assembly 21

37 6.8 Online software and Trigger 22

38 6.9 Offline software - detector simulation, geometry, offline tracking 24

39 **7 Organization and Collaboration** **25**

40 **8 Schedule and Cost Baseline** **26**

41 8.1 Schedule 26

42 8.2 Cost 27

43 8.3 Resources 28

44 8.4 Milestones 28

| | | |
|----|--|-----------|
| 45 | 8.5 Major Cost Items | 28 |
| 46 | Supplemental Materials: | 30 |
| 47 | 9 Project Timeline, Deliverables, and Tasks | 30 |
| 48 | 10 Abbreviations and Code Names | 35 |
| 49 | 11 Literature Cited | 36 |

Abstract

Title: A Monolithic-Active-Pixel-Sensor-based Vertex Detector (MVTX) for the sPHENIX Experiment at RHIC

Lead Institution: Los Alamos National Laboratory

Principal Investigator: Ming X. Liu

Co-Investigators: Grazyna Odyniec (LBNL) and Robert Redwine (MIT)

The goal of the sPHENIX experiment at the Relativistic Heavy Ion Collider (RHIC), which was granted DOE CD-0 recently, is to study the microscopic nature of the quark-gluon-plasma that is believed to have existed a few microseconds after the Big Bang, filling the entire universe at a temperature of several trillion Kelvin. Measurements at the Relativistic Heavy Ion Collider at Brookhaven National Laboratory (BNL) and the Large Hadron Collider (LHC) at CERN have both confirmed the existence of the QGP. The QGP created in heavy nuclei collisions at very high energy has been seen to have novel emergent properties, such as very low viscosity close to the quantum limit. The ultimate goal for understanding the strong interaction under extreme conditions is to develop a microscopic description of this plasma, including an understanding of the origin of its thermodynamic properties. Measurements of hadronic jets will reveal the internal structure of the QGP via their scattering with quasi-particles in the medium. Bottom quark jets (*b*-jets) and B-mesons produced in heavy ion collisions at RHIC offer a unique set of observables due to the large bottom quark mass, but need to be measured across an unexplored kinematic regime. These measurements of *b*-jets and B-mesons are essential to produce a complete understanding of the plasma. sPHENIX is a state-of-the-art jet detector designed to collect a suite of unique jet observables with unprecedented statistics. Reconstruction and identification of *b*-jets and B-mesons requires both precision tracking of charged particles close to the beam collision point and high detection efficiency. We propose to build a Monolithic-Active-Pixel-Sensor based precision vertex detector (MVTX) to ensure the sPHENIX inner tracker is capable of performing these key measurements.

1 Executive Summary

sPHENIX is a next-generation nuclear physics experiment providing world-class capabilities for multi-scale studies of the strongly coupled quark gluon plasma (QGP), planned for the Relativistic Heavy Ion Collider (RHIC) at Brookhaven National Laboratory in 2022 and beyond. The need for these capabilities to advance our understanding of the origins of novel QGP properties is detailed in the 2015 NSAC Long Range Plan.

Precise measurements of heavy flavor-tagged jets and B-hadron nuclear modification and flow in heavy ion collisions are key scale-dependent observables. Measuring these rare observables demands high precision tracking with excellent displaced secondary vertex capabilities. While the baseline sPHENIX detector anticipates a small aperture detector for secondary vertexing, exploiting the full potential of heavy flavor QGP signatures, and optimizing the use of RHIC luminosity and available running time, is only possible with a large acceptance precision vertex detector. We propose to build a thin, extremely precise silicon pixel vertex detector for the sPHENIX experiment to enable these key measurements. The detector will be based closely on the latest generation of Monolithic-Active-Pixel-Sensor (MAPS) technology, developed for the ALICE collaboration at CERN, and leveraging the extensive R&D investments made in this technology over a period of several years. Last summer, the Los Alamos National Laboratory High-Energy Nuclear Physics Group was awarded an internal LDRD grant (\$5M over 3 years, FY17-19) to develop a state of the art MAPS-based telescope to demonstrate the tracking capability of such a device for the sPHENIX experiment. The LANL LDRD will allow us to carry out the much needed early R&D for the MAPS readout electronics and produce the initial conceptual design of mechanical system integration into the sPHENIX detectors, and also develop a state of the art theoretical calculation, modeling and full physics simulations and analyses with a realistic detector configuration.

The MAPS-based Vertex Detector (MVTX) is proposed to be ready for Day-1 sPHENIX data taking. This detector will provide world-class scientific results in key areas encompassed by the DOE Nuclear Physics mission. It will allow U.S. scientists to make fundamental inquiries into the nature of the QGP that cannot be probed with other existing facilities worldwide. In particular, the sPHENIX experiment, which was granted with DOE CD-0 in September 2016, will complement and extend the ongoing and future QGP studies at RHIC and LHC, and will become the next generation U.S. flagship high energy nuclear physics program at the DOE's key facility in this field.

2 Physics Goals

The physics goals of the proposed vertex detector project are aligned with the key challenges and physics opportunities outlined in the 2015 NSAC Long-Range Plan: “There are two central goals of measurements planned at RHIC, as it completes its scientific mission, and at the LHC: (1) Probe the inner workings of QGP by resolving its properties at shorter and shorter length scales. The complementarity of the two facilities is essential to this goal, as is a state-of-the-art jet detector at RHIC, called sPHENIX. (2) Map the phase diagram of QCD with experiments planned at RHIC.”

The key approach for goal (1) is microscopy of the QGP through probes that are sensitive to characteristic scales in the plasma. The baseline sPHENIX design is optimized to employ light quark and gluon jets over a wide kinematic range and Upsilon’s as such scale-sensitive probes. The vertex detector described in this proposal will greatly expand the sPHENIX capabilities in an additional dimension related to scales in the QGP, by allowing a range of precision studies as a function of parton mass. Studies of heavy-flavor hadrons have been a focus of recent upgrades in PHENIX and STAR at RHIC. These studies, as well as new measurements by the current LHC experiments form the key motivation for the ALICE Phase-I upgrades for the early 2020’s. In combination with the large acceptance and high rate capability of sPHENIX, the vertex detector upgrade provides access to observables that are not accessible with the present RHIC detectors and are complementary to those at LHC.

Heavy flavor quarks (c , b) play a unique role for studying the QCD in vacuum as well as at finite temperature or density. Their masses are much larger than the QCD scale (Λ_{QCD}), the additional QCD masses due to chiral symmetry breaking, as well as the typical medium temperature created at RHIC and LHC. Therefore they are created predominantly from initial hard scatterings and their production rates are calculable in perturbative QCD. They are thus calibrated probes that can be used to study the QGP in a controlled manner.

The vertex detector will enable a wide range of heavy-flavor studies, extending present RHIC measurements to significantly larger transverse momenta, and provide access to qualitatively new QGP signatures. A particular new capability, in combination with the sPHENIX calorimetric jet reconstruction, is the identification of jets originating from heavy quarks. In this proposal, we will use the measurements of b-tagged jets as a case study to illustrate the new capabilities the upgrade brings to RHIC and the overall field. This particular measurement represents both a new opportunity at RHIC and an example of complementarity to the LHC: the projected sPHENIX measurement both extends the LHC measurement to lower transverse momenta and provides a kinematic overlap, where the same jets can be studied in the different QGP conditions at RHIC and LHC.

2.1 B -meson physics at low p_T

As first revealed by the single-electron nuclear modification factor R_{AA} data at RHIC, heavy quarks lose energy when traversing the QGP medium through both radiative mechanism as well as elastic collisional mechanism [1, 2]. Recent Charm-hadron data from RHIC and LHC show their R_{AA} are quite similar to those of light flavor hadrons [3, 4]. Theoretical calculations predict that Bottom-hadrons should be much less suppressed compared to charm and light flavor hadrons due to the much larger bottom quark mass in the p_T region of 5-20 GeV/ c at RHIC [5]. To systematically understand the flavor/mass dependence of parton energy loss mechanism, the next physics goal would be to measure and understand the bottom hadron production in heavy ion collisions.

Another unique feature of heavy quarks is that their propagation inside the QGP medium can be treated in analogy to Brownian motion” when their masses are much larger than every momentum kick they suffer in the QGP. Therefore, one can simplify their dynamics in the QGP with a Langevin simulation and then access the heavy quark spatial diffusion coefficient ($2\pi TD_s$), the relevant QGP medium transport parameter,

149 by comparing data and model calculations. Recent STAR HFT measurements reveal that the Charm-hardon
150 v_2 follows the same empirical $(m_T - m_0)$ scaling as light hadrons at $p_T < 4 \text{ GeV}/c$ [6]. This suggests charm
151 quarks may have reached the thermal equilibrium. On the other hand, theoretical calculation also shows
152 the Langevin simulation for charm quarks may have sizable corrections compared to the full Boltzmann
153 transport [7]. To precisely determine the intrinsic QGP transport parameter, D_s , measurements of bottom
154 hadron production, particularly at low p_T , will be critical.

155 Furthermore, measuring the total bottom cross section in heavy ion collisions will be crucial for the
156 interpretation of the suppression in the bottomonia production, which is one of the highlighted sPHENIX
157 measurements that has been proposed.

158 **2.2 b -jet physics at intermediate p_T**

159 Compared to single hadrons, measurements of jets provide more information on the initial parton kine-
160 matics and the nature of parton interactions with the QGP medium. The evolution of parton showers probes
161 the coupling with the medium over a range of scales, providing sensitivity to its scale-dependent micro-
162 scopic structure. Jets containing b-quarks are of particular interest, as Bottom quarks, which are ~ 1000
163 times heavier than the light quarks, produce unique energy loss signatures due to their large mass (4.2
164 GeV/c^2). At momenta comparable to this scale, bottom quarks will preferentially lose energy via collisions
165 with the plasma quasi-particles and not via gluon radiation, which is predominant for light quarks.

166 Jets containing b -quarks are also distinct from light-quark jets in their high multiplicity and hard frag-
167 mentation, where the leading particle typically carries 70-80% of the jet energy. Measurements of b -jets in
168 Pb+Pb collisions at LHC cover momenta larger than $80 \text{ GeV}/c$. Surprisingly, these measurements indicate a
169 nuclear modification factor very similar to inclusive jets [8]. One of the explanations is that the mass of the
170 quark is irrelevant for a $80 \text{ GeV}/c$ jet. The other hypothesis is that given that most of b -jets at LHC are from
171 gluon splitting processes, the jet containing a b -quark still behaves as a massive color octet object when
172 crossing the medium, resembling a massive gluon [9]. These ambiguities can be resolved at RHIC energies
173 since

- 174 1. b -jets can be measured with momentum as low as $15 \text{ GeV}/c$, where the quark mass is more important
175 for the energy loss mechanisms
- 176 2. the main process producing b -jets at RHIC is the leading order gluon fusion ($g + g \rightarrow b + \bar{b}$) and
177 excitation of intrinsic b -quarks in the proton wave function ($b + g \rightarrow b + g$). The b -quark produced in
178 these processes crosses the medium as a massive quark (color triplet state).

3 Detector Requirements

The planned sPHENIX detector [10, 11] is designed to perform measurements of jets, quarkonia in $p+p$ and heavy ion collisions at RHIC. The baseline sPHENIX detector consists of a tracking system and a calorimeter system, both of which have full 2π acceptance in azimuth and a pseudorapidity coverage of $|\eta| < 1$ and is assembled around a 1.4 Tesla superconducting magnet coil. The sPHENIX calorimeter system includes an electromagnetic calorimeter and an inner hadronic calorimeter, which sit inside a solenoid coil, and an outer hadronic calorimeter located outside of the coil. The baseline tracking system includes a strip intermediate silicon tracker (INTT) and an outer time projection chamber (TPC) and allows addition of an inner vertex tracker.

The sPHENIX baseline detector allows calorimetry based triggering and measurement of jets at RHIC with an energy resolution of $\Delta E/E = 120\%/\sqrt{E}$ and provides containment for 80% of opposite di-jet pairs from the same hard collision. The electromagnetic calorimeter provides for the triggering, identification and measurement of high-energy electrons with an energy resolution better than $\Delta E/E = 15\%/\sqrt{E}$. The tracking momentum resolution is 1-2% in the transverse momentum range of 0-10 GeV/ c , which allows reconstructing Upsilon invariant mass resolution of < 100 MeV/ c^2 . The DAQ system is designed to provide calorimetry-based trigger on jets and Upsilon signals, and to record full detector events at 15 kHz, which matches the collision rate delivered by RHIC within a vertex range of $|z| < 10$ cm.

3.1 Physics-driven detector requirements for MVTX

In order to deliver the desired physics goals with b -jets and B -mesons, requirements are placed on the detector design in the following aspects:

- **Acceptance:** both b -jet and B -meson physics programs are statistics-limited. Therefore, the inner tracking detector should match the acceptance for the planned sPHENIX detector in order to provide a precision vertex displacement measurement for all tracks detected by sPHENIX. The detector should have full coverage of $|\eta| < 1$ for charged tracks with hits in at least two MVTX layers for events within $|z| < 10$ cm.
- **Event rate:** the b -jet physics program requires sampling a large number of events with inclusive jets and the B -meson physics program requires high statistics minimum biased Au+Au collision events. Since both programs are statistics-limited, the inner tracker should deliver an event rate not lower than the sPHENIX trigger rate of 15 kHz.
- **DCA resolution:** The $c\tau$ for D and B decays is about $120 \mu\text{m}$ and $460 \mu\text{m}$, respectively, and the Distance of Closest Approach (DCA) with respect to the primary vertex of these heavy-flavor mesons is larger than prompt particles. Therefore it is crucial to have a good DCA resolution ($< 50 \mu\text{m}$ at $p_T > 1$ GeV/ c) to distinguish tracks from heavy flavor hadron decay. In order to achieve the required DCA resolution down to $p_T > 1$ GeV/ c , where multiple scattering is dominant, it is very important to reduce the material budget of the inner tracking detector.
- **Efficiency:** The b -jet physics program requires simultaneous detection of several displaced vertex tracks from B -meson decay within the jet; the B -meson physics program requires detection of both of the decay particle tracks from the $B \rightarrow D \rightarrow \pi^\pm K^\mp$ decay chain. Therefore, good tracking efficiency is required, i.e. a minimal efficiency 60% at $p_T = 1$ GeV/ c in central Au+Au collisions in order to deliver the minimal purity and efficiency for b -jet tagging.

These requirements are summarized in Table 1.

| Item | Requirement |
|---------------------|--|
| Acceptance | Vertex $ z < 10$ cm, $ \eta < 1$, full azimuthal coverage |
| Event rate | Matching the sPHENIX DAQ rate of 15 kHz event rate |
| DCA resolution | $< 50 \mu\text{m}$ for charged pions at $p_T = 1 \text{ GeV}/c$ |
| Tracking efficiency | $> 60\%$ efficiency for charged pions at $p_T = 1 \text{ GeV}/c$ in central Au+Au collisions |

Table 1: Summary for the vertex detector requirements

4 Technology Choices and Detector Layout

We propose to adopt the ALICE Inner Tracking System (ITS) Upgrade 3-layer MAPS-based Inner Barrel (IB) detector design, with minimal modifications to both electrical and mechanical systems, for use in the sPHENIX experiment. A full description of the ITS Upgrade can be found in the Technical Design Report [12].

Figure 1 shows the side view of ALICE ITS IB mounted on the sPHENIX beam pipe. Sitting outside of the MVTX is the intermediate silicon strip tracker (INTT) planned to be funded by the RIKEN research institute in Japan. With single-event response and spatial resolution between that of the MVTX detector and that of the TPC, the INTT is intended to support pattern recognition and data-driven calibrations in heavy ion and $p+p$ collisions. The precise geometry and configuration of the INTT is being optimized, and that effort is not part of this proposal.

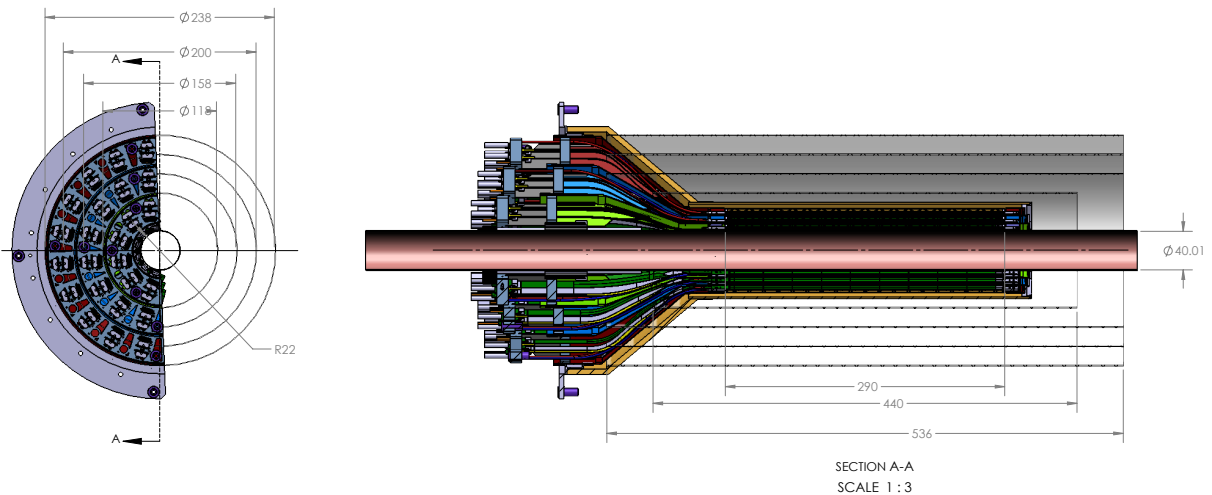


Figure 1: Side view of MVTX, showing its location relative to the sPHENIX beam pipe. All services come from one end (left side), including analog and digital power, cooling lines and high-speed Firefly data cables.

4.1 Design goals and technology choice

Recent developments in the technology of Monolithic-Active-Pixel-Sensors (MAPS) have made it possible to have sensor designs with high speed readout, fine granularity, minimal radiation length and low

234 power, all at relatively low cost. The ALPIDE sensor [13, 14] developed for the ALICE ITS Upgrade has
235 attributes that meet the sPHENIX requirements. We have focused our design on leveraging the extensive
236 R&D work already done for the ALICE ITS. We intend to use the design of the inner three layers of the AL-
237 ICE ITS as the primary baseline design for the sPHENIX MVTX vertex detector, providing the basis for the
238 designs and work plans in this proposal. On the basis of the requirements and considerations of Section 3,
239 the proposed solution for the layout of the sPHENIX vertex detector is a 3-layer silicon barrel based on
240 the technology of Monolithic Active Pixel Sensors. The main design considerations to meet the necessary
241 capabilities in terms of displaced vertex resolution, tracking efficiency and readout rate, are summarized
242 here:

- 243 • The track pointing resolution is mainly determined by the two innermost measurements of the track
244 position. This requires the first detection layer be as close to the beam line as possible. Three layers
245 provide redundancy against failure of detector modules. The radial distance between the three layers
246 should be as small as possible, to preserve the two innermost measurements of the track position if
247 one of the points close to the primary vertex is not attached to it.
- 248 • Reduction of the material budget to minimize multiple-scattering track distortion. Reducing the ma-
249 terial budget of the first detection layer is particularly important for improving the impact parameter
250 resolution.
- 251 • The segmentation of the detector determines the intrinsic spatial resolution of the reconstructed track
252 points. Excellent spatial resolution of the first layer is key for the resolution of the impact parame-
253 ter at high particle momentum where the effect of the multiple scattering becomes negligible. Fine
254 segmentation is also important to keep the occupancy low.
- 255 • Short integration time window to minimize the event pile-up and keep the occupancy at a low value
256 when reading out the detector at the expected rate of 15 kHz.

257 These design goals lead to a vertex detector configuration consisting of three concentric layers of pixel
258 detectors. Monolithic Active Pixel Sensors implemented using the 0.18 μm CMOS TowerJazz technology
259 and developed by the ALICE collaboration at CERN are an ideal technology for the three layers. The basic
260 active MVTX element is the Pixel Chip. It consists of a single silicon die of about 15 mm x 30 mm, which
261 incorporates a high-resistivity silicon epitaxial layer (sensor active volume), a matrix of charge collection
262 diodes (pixels) with a pitch of about 30 μm , and the electronics that perform signal amplification, digitization
263 and zero-suppression. Only the information on whether or not a particle crossed a pixel is read out. The
264 main functional elements of the sPHENIX MVTX detector are introduced in the following section, while its
265 main geometrical parameters are listed in Table 2.

266 4.2 Detector layout

267 The proposed sPHENIX MVTX detector is designed to leverage the extensive research and development
268 behind the design of the ALICE ITS Upgrade Inner Barrel. In the ALICE design, the layers are azimuthally
269 segmented in units called staves, which are mechanically independent. Staves are fixed to a support structure,
270 half-wheel shaped, to form half-layers. The stave and the half-layer are shown in Figure 2).

271 The term *stave* will be used to refer to the complete detector element. It consists of the following main
272 components:

- 273 • Space Frame: a truss-like lightweight mechanical support structure for the single stave based on
274 composite material (carbon fiber).

| | Layer 0 | Layer 1 | Layer 2 |
|--------------------------------|---------|---------|---------|
| Radial position (min.) (mm) | 22.4 | 30.1 | 37.8 |
| Radial position (max.) (mm) | 26.7 | 34.6 | 42.1 |
| Length (sensitive area) (mm) | 271 | 271 | 271 |
| Active area (cm ²) | 421 | 562 | 702 |
| Number of pixel chips | 108 | 144 | 180 |
| Number of staves | 12 | 16 | 20 |

Table 2: Parameters of the sPHENIX MVTX design.

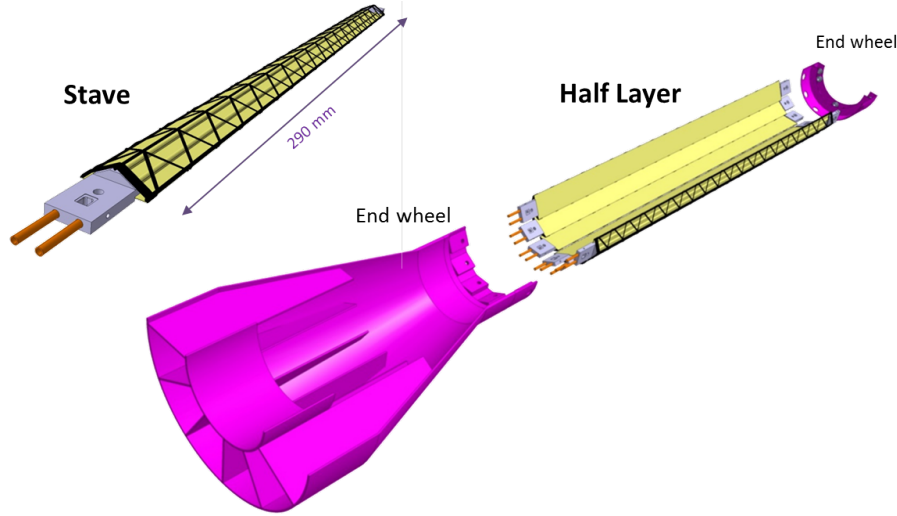


Figure 2: MVTX Stave and Half-Layer: each half-layer is composed of a set of staves fixed to wheel-shaped support structures. The layout shown here is based on the ALICE ITS Upgrade Inner Barrel design.

- 275 • Cold Plate: carbon ply that embeds the cooling pipes.
- 276 • Hybrid Integrated Circuit (HIC): assembly consisting of the polyimide flexible printed circuit (FPC)
- 277 on which nine Pixel Chips and some passive components are bonded.

278 Each stave will be instrumented with one HIC, which consists of a row of nine Pixel Chips glued and
279 connected to the FPC, hence covering a total active area of 15 mm x 271.2 mm including the 150 μ m gap
280 between adjacent chips along z. The interconnection between Pixel Chips and FPC is achieved via wire
281 bonding. The HIC is glued to the Cold Plate with the Pixel Chips facing it in order to maximize cooling
282 efficiency. An extension of the FPC connects the stave to a patch panel that is served by the electrical
283 services entering the detector from one side only. A mechanical connector at each end of the stave allows
284 the fixation and alignment of the stave itself on the end-wheels, as described in Section 6.3. The inlet and
285 outlet of the closed-loop cooling circuitry are located at the same end of the stave because the cooling is also
286 served from the same side as all other services. The prototyping of the stave is well advanced. The design
287 of the stave accounts for the tight requirement on the material budget, which is limited to 0.3% X_0 .

288 The three layers are then integrated together and with an outer cylindrical structural shell (CYSS) to
289 form two detector half barrels, as shown in Figure 3).

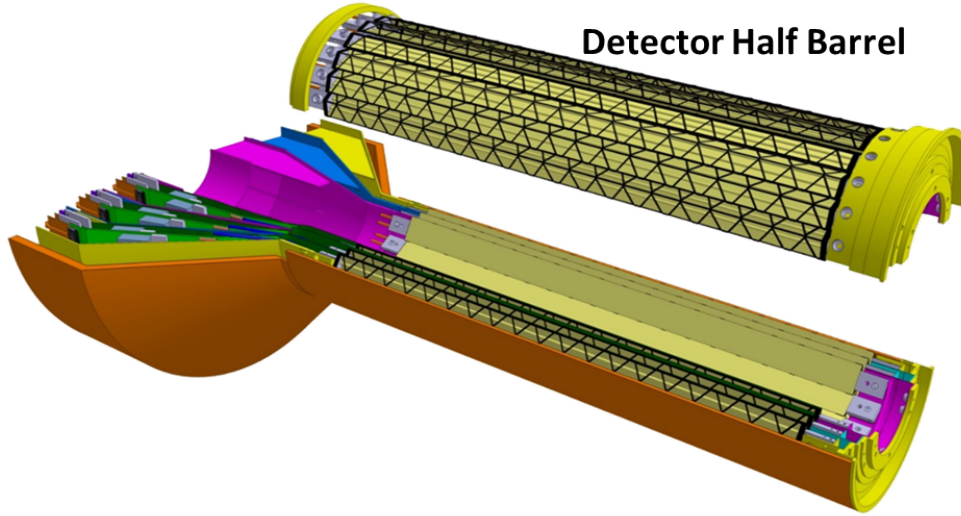


Figure 3: MVTX 3-layer Detector Barrel: each half-barrel is composed of a detector section and a services section. The layout shown here is based on the ALICE ITS Upgrade Inner Barrel design.

5 Physics Performance

We discuss the expected tracking performance of the MVTX in the sPHENIX experiment. The MVTX is the key device in sPHENIX to provide the precision measurement of the primary vertex as well as the displaced secondary tracks from heavy quark decays. Figure 4 shows the single track efficiency and the DCA pointing resolution in the bending plane as a function of p_T based on the full GEANT4 detector simulation plus the offline tracking software reconstruction (see Section 6.9 for offline simulation and tracking). The efficiencies were evaluated using charged pion tracks embedded in central (i.e., high multiplicity) HIJING events. The single track efficiency is about 80% at 1 GeV/c and the DCA pointing resolution is about $40 \mu\text{m}$ for 0.5–1 GeV/c tracks. These performance parameters meet detector requirements based on the full detector simulation study.

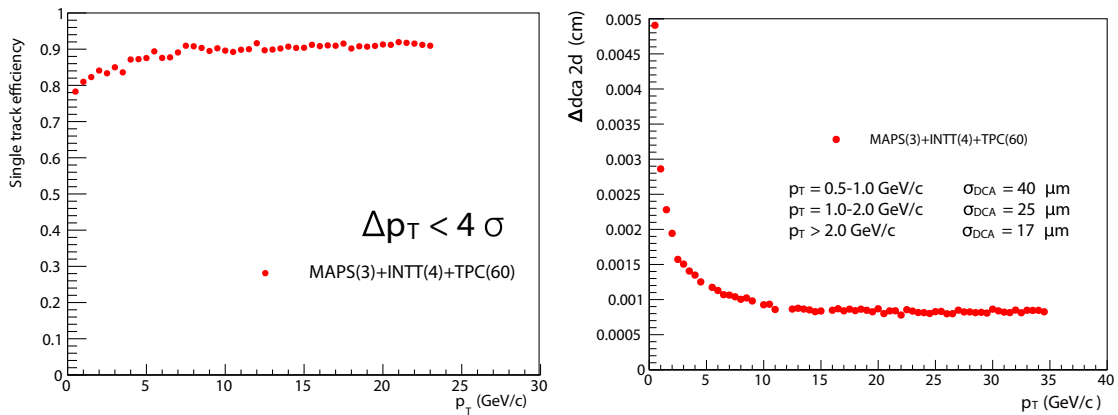


Figure 4: Single track reconstruction efficiency (left) and DCA pointing resolution in the bending plane (right) in central Au+Au collisions from full HIJING plus GEANT4 simulation.

299 5.1 *b*-jet tagging

300 Detection of *b*-jets with the sPHENIX detector is complicated by the comparative rarity of *b*-jets, as
 301 shown in Figure 5, and also by the significant background of the underlying event in heavy ion collisions.
 302 Multiple exploratory methods have been developed to demonstrate that the proposed MVTX detector allows
 303 *b*-jet tagging in sPHENIX and to enable cross checks of the expected systematic uncertainties. As shown in
 304 the right diagram of Figure 6, these methods are based on the unique features of *B*-hadron decays, including
 305 the finite decay length and leptonic decay products. These methods are:

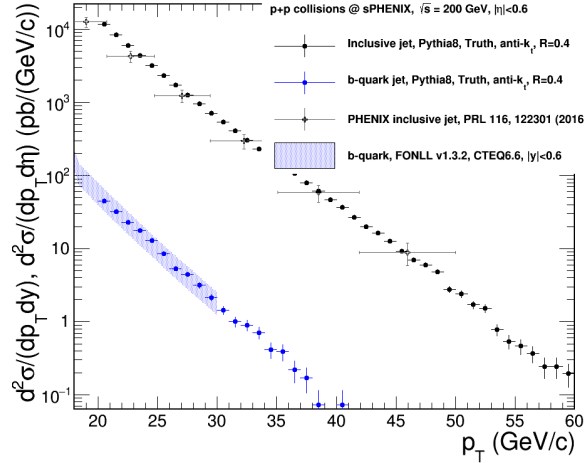


Figure 5: Comparison of the cross section for *b*-jets (blue) and all jets (black). *b*-jets are rare compared to the much more abundant light quark jets.

- 306 • Identify *b*-jets by requiring multiple tracks within the jet cone that do not originate from the primary
 307 collision vertex. These are likely be the long-lived *B*-hadron decay products. As an initial study,
 308 we performed a full sPHENIX detector simulation to demonstrate such capability in *p*+*p* collisions
 309 as shown in the left side panels of Figure 7 and 8. Despite the simplified algorithm used in this
 310 exploration, the *b*-tagging performance approaches that seen by CMS in their *b*-jet analysis at much
 311 higher energy [8, 15]. Additional techniques will be deployed in the final software package to further
 312 optimize performance, including likelihood analyses, 3-dimensional track displacement and machine
 313 learning techniques.
- 314 • Identify *b*-jets by requiring that multiple tracks within the jet cone come from the same displaced sec-
 315 ondary vertex distinct from the primary vertex. This method is related to the previous one; however it
 316 also uses the knowledge that a *B*-hadron is likely to decay into multiple daughter particles. This pro-
 317 vides additional power in selecting and cross checking *b*-jet candidates identified via the first method.
 318 We also demonstrated this method in full simulation as shown in the right panels of Figure 7 and 8.
 319 This method also provide data driven quantification of *b*-jet purity via secondary vertex kinematics
 320 fitting.
- 321 • Identify *b*-jets by requiring that electron or positron tracks are detected within the originally identified
 322 jet cones. Utilizing the fact that *B*-hadrons have a significant chance (20%) to decay to a leptonic final

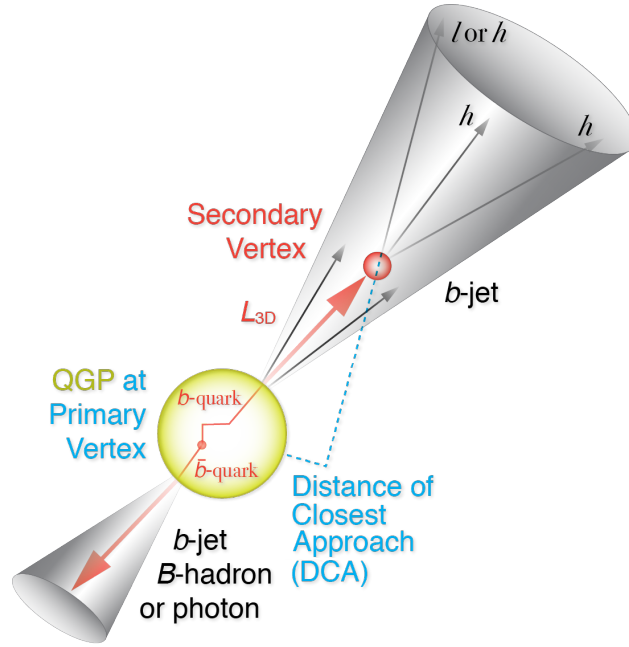


Figure 6: A b -quark traverses the QGP and fragments into a b -jet. The principles of tagging the rare b -jets are based on unique features of B -hadrons: long life time and finite decay length of B -hadron ($L_{3D} \sim \text{few mm}$), decay tracks from secondary vertices and leptonic decay products.

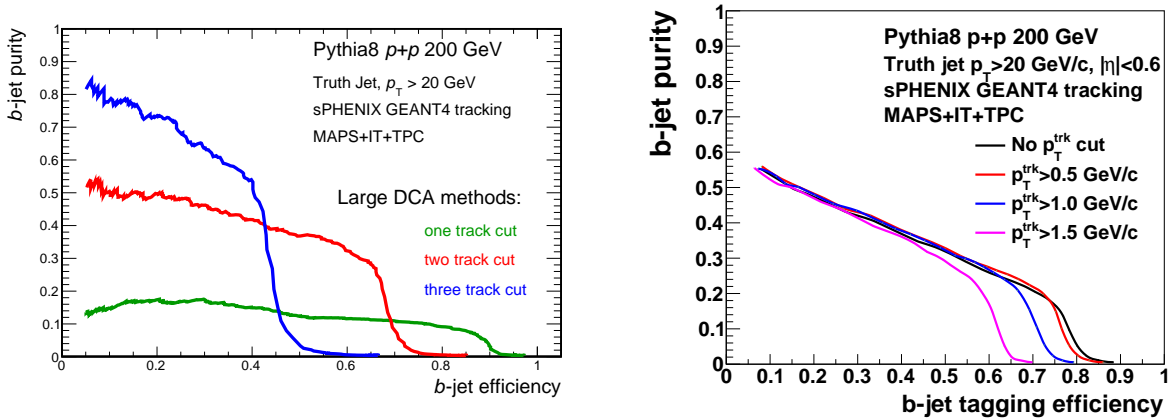


Figure 7: Projected b -jet tagging performance study in $p+p$ collisions using the multiple large DCA track method on the left panel and secondary vertex method as on the right panel.

323 state, this is a nearly orthogonal method that could provide an independent cross check of both meth-
 324 ods above. We will explore its feasibility in the sPHENIX environment and performance projections
 325 for such cross checks.

326 After the initial identification of b -jet candidates, the purity of b -jets in the candidate sample will be
 327 quantified in a data-driven way using the invariant mass and transverse momentum of the secondary vertex,
 328 which has proven to be critically important in the LHC environment [8, 15]. The projected uncertainty of
 329 the nuclear modification of inclusive b -jet is shown in Figure 9, which places stringent tests on the models

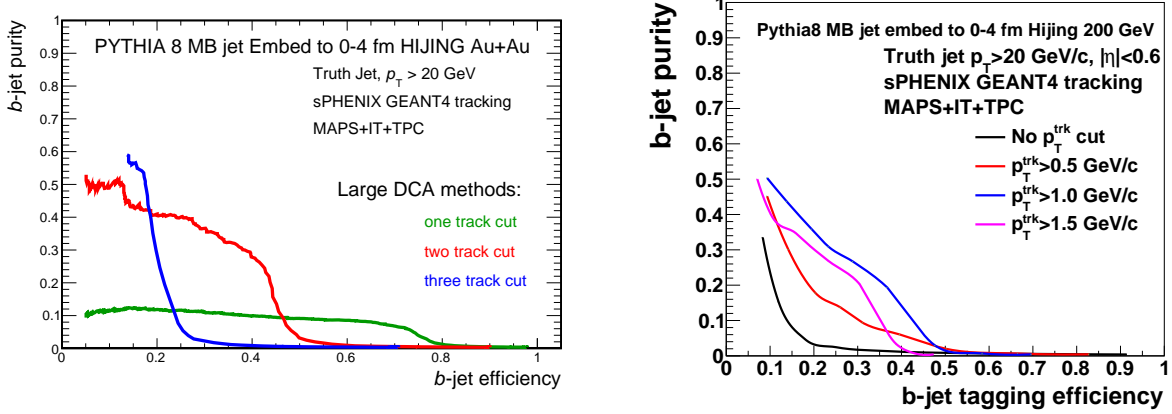


Figure 8: Preliminary projection of b -jet tagging performance study in Au+Au collisions using the multiple large DCA track method on the left panel and secondary vertex method as on the right panel. The tracking and tagging software is not yet fully optimized. Nevertheless, the performance curves allow an analysis working point of 30-40% purity at 30-40% b -jet efficiency as used in the existing analysis performed at LHC energy [8].

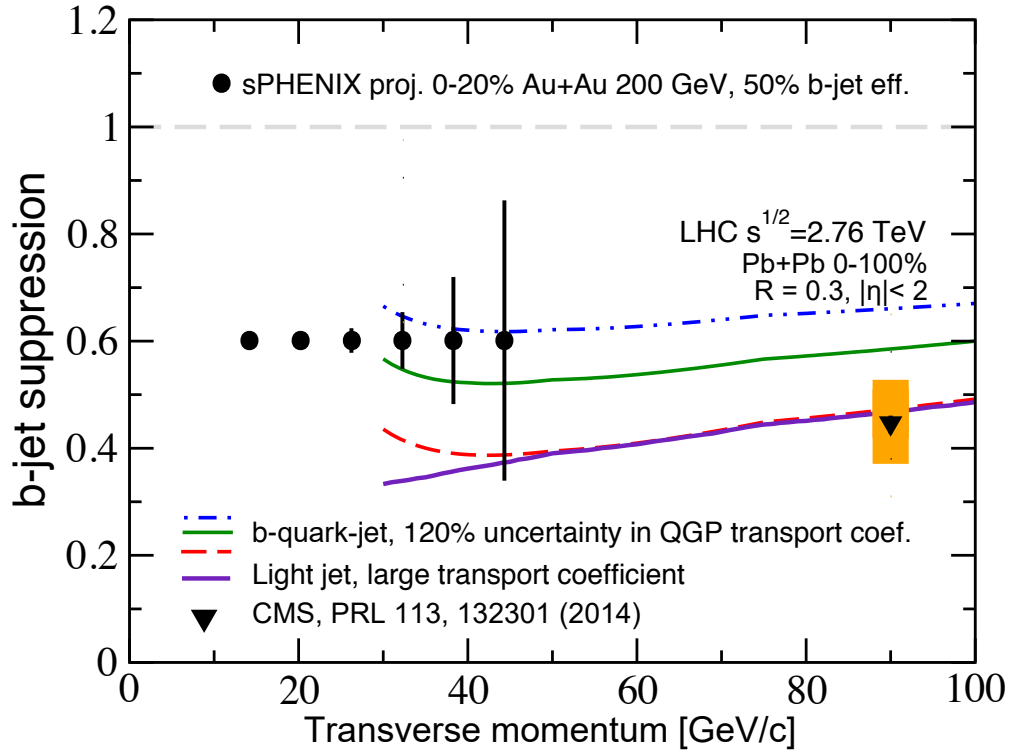


Figure 9: Projection of sPHENIX inclusive b -jet data in terms of the nuclear suppression factor (black circles), which is compared with CMS data (black triangles) [8], and QGP transport models for b -quark jets evaluated at the LHC energy (curves) [9]. sPHENIX with the proposed MVTX detector will bring new data to RHIC energy and to the 15-40 GeV/ c transverse momentum region in which b -quarks move slowly and are predicted to show strong deviations from light quark jets. The inclusive b -jets at RHIC energy are expected to be dominated by b -quark jets [16]. The proposed b -jet substructure and correlation studies will also enhance the selection of b -quark jets (See text for details).

330 describing the coupling between heavy quarks and the QGP [9]. We are in close collaboration with theory
 331 groups to update the model predictions of inclusive b -jet nuclear modification at the RHIC energy in the
 332 sPHENIX kinematic region.

333 Beyond the inclusive b -jet nuclear modification measurement, additional techniques in jet substructure
 334 and correlation studies will be enabled by the MVTX detector. Inclusive b -jets can originate from a high-
 335 energy b -quark (a true b -quark jet) or from a gluon that splits into b -quark and b -antiquark ($g \rightarrow b\bar{b}$ -jet).
 336 These two categories of b -jets could potentially have very different interactions with the QGP, because in
 337 the latter case the correlated b -quark and b -antiquark traverse coherently through the QGP in a color octet
 338 state with twice the b -quark mass [9]. Although inclusive b -jets at RHIC are expected to be dominated by
 339 the b -quark jets [16], the remaining $g \rightarrow b\bar{b}$ -jet component could complicate the interpretation the inclusive
 340 b -jet results. The MVTX detector will allow us to discriminate these two categories of b -jet productions and
 341 provide cleaner access to the dynamics of high energy b -quark interactions with the QGP:

- 342 • Correlation studies for b -jets: the fraction of true b -quark jets can also be enhanced by selecting b -
 343 quark partonic production channels. This is achieved by requiring the b -jet candidate to be correlated
 344 with another b -jet, B -hadron, or photon in the same event [17], as illustrated in Figure 6. In particular,
 345 correlations between two b -jets can be measured with high statistics using the MVTX and sPHENIX
 346 detectors, taking advantage of their high rate capability and their large instrumented acceptance (cov-
 347 ering nearly 80% of produced di-jets). A preliminary projection of the transverse momentum balance
 348 of b -jet pairs is shown in Figure. 10, which is comparable in precision with a recent results from
 349 Pb+Pb collision at $\sqrt{s_{NN}} = 5.02$ TeV measured by the CMS collaboration [15].
- 350 • Jet substructures: in recent years, the field of high-energy physics has developed a set of techniques
 351 to inspect the substructure of jets, to tag boosted objects and to differentiate between gluon and quark
 352 jets. These techniques have recently been adopted to study the interplay between light-jet probes with
 353 the QGP medium at the LHC [18] and at RHIC [19]. These techniques can also be utilized in identi-
 354 fying true b -quark jets for sPHENIX. Specifically, so-called jet grooming algorithms will be used to
 355 remove soft radiation from the jet, and to identify two leading subjet structures that correspond to the
 356 earliest splitting of the initiating parton [20]. In the leading order picture, the transverse momentum
 357 of the two subjets is likely be similar in a $g \rightarrow b\bar{b}$ -jet, and in true b -quark jets, one subjet would likely
 358 dominate. Therefore, a measurement of transverse momentum ratio of the two subjets will be used
 359 to identify and quantify the purity of the true b -quark jets. A secondary vertex that is found by the
 360 MAPS detector that associates with the subjets can further confirm the b -quark origin of the subjets.

361 5.2 B -meson tagging

362 B -meson production can be studied through either inclusive decay daughters, e.g. D -mesons, J/ψ or e^\pm
 363 via the impact parameter method or exclusive reconstruction, e.g. $D + \pi$ or $J/\psi + K$ etc via the secondary
 364 vertex reconstruction. These channels offer the sensitivity to access the low- p_T B -mesons. The fast MAPS
 365 silicon detector can efficiently separate the B -meson decay signals from the background dominantly coming
 366 from the primary interaction vertex in heavy-ion collisions.

367 One major challenge for separating low- p_T B -meson decays from the primary vertex are the background
 368 tracks that come from the primary heavy-ion collisions. In the following, we will discuss the B -meson signal
 369 significance in the non-prompt D^0 channel using the full GEANT4/tracking simulation + a fast Monte Carlo
 370 method. The GEANT4/tracking simulation includes the tracking efficiency together with the MAPS detector
 371 plus the full DCA distributions of the charged tracks pointing to the primary vertex. These are fed into a

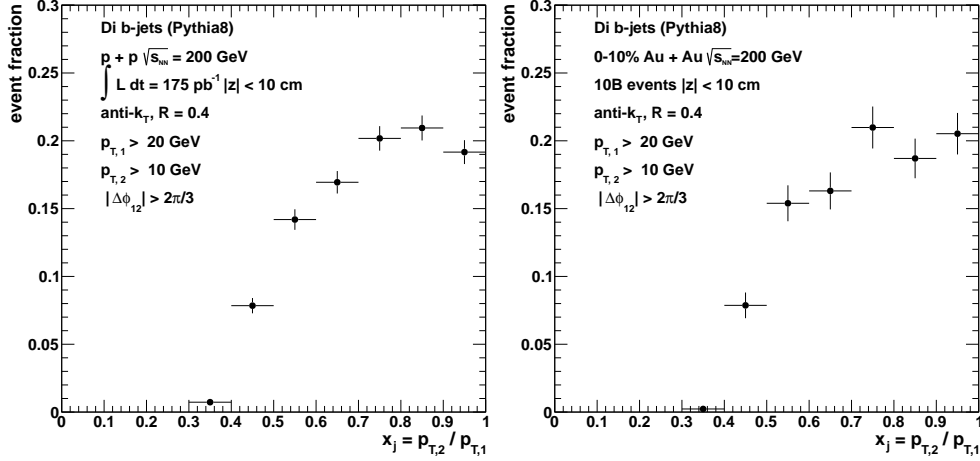


Figure 10: Preliminary projection of transverse momentum balance of b -jet pairs as enabled by the MVTX detector, for $p+p$ (left) and for 0-10% central Au+Au collisions at $\sqrt{s_{NN}} = 200$ GeV.

372 fast Monte Carlo simulation that can be conducted with sufficient statistics for both signal and background
 373 evaluations.

374 Figure 11 left plot shows the D^0 DCA distributions to the primary vertex in the p_T range of 4-5 GeV/ c
 375 for 100M 0-10% central Au+Au events. The narrow peak close to zero indicates the prompt D^0 signal
 376 from the primary collisions. The red distribution presents the signals from B -meson decays. The estimated
 377 background contribution is also shown in the same plot as the blue histograms.

378 Figure 11 right plot shows the estimated prompt and non-prompt D^0 significance as a function of p_T
 379 for 10 billion 0-10% central Au+Au collisions at $\sqrt{s_{NN}} = 200$ GeV taken with the sPHENIX and MVTX
 380 detectors. The red squares are estimated non-prompt D^0 significance with an additional Time-Of-Flight
 381 (TOF) detector for particle identification. The TOF detector assumed here has a timing resolution of 40ps
 382 or less which allows clean pion/kaon separation up to 1.6 GeV/ c .

383 The prompt D^0 production rate is taken from existing STAR measurements[6] and the B -meson produc-
 384 tion rate is based on the FONLL pQCD calculation in $p + p$ collisions and scaled with number-of-binary
 385 collisions to central Au+Au collisions. The estimation shows good performance for B -meson tagging using
 386 the non-prompt D^0 in a wide p_T region. The additional TOF detector would enhance the non-prompt D^0
 387 measurement especially in the low p_T region. Particle identification capability will be greatly enhanced
 388 should the TOF be realized, and so will be the the overall physics program at sPHENIX.

389 We take the above significance estimation and convert to the statistical uncertainties on the physics
 390 observables - nuclear modification factor R_{CP} and v_2 for 100 billion Au+Au 200 GeV events, shown in
 391 Fig. 12. The left figure clearly shows that one can separate the non-prompt D^0 R_{CP} from the prompt D^0
 392 provided the suppression hierarchy predicted by theory calculations [5, 21, 22] holds. In the right figure, the
 393 estimated uncertainty shows that one can clearly answer the question whether bottom quarks flow with the
 394 medium or not. Such a precision should allow further joint efforts between theorists to further constrain the
 395 heavy quark diffusion coefficient, the intrinsic transport parameter of the sQGP.

396 The performance described above has been focused on the inclusive non-prompt D^0 channel. Simu-
 397 lations have been pursued to continue exploring the B -meson tagging using non-prompt J/ψ 's or further
 398 exclusive reconstruction of B -meson through hadronic decays.

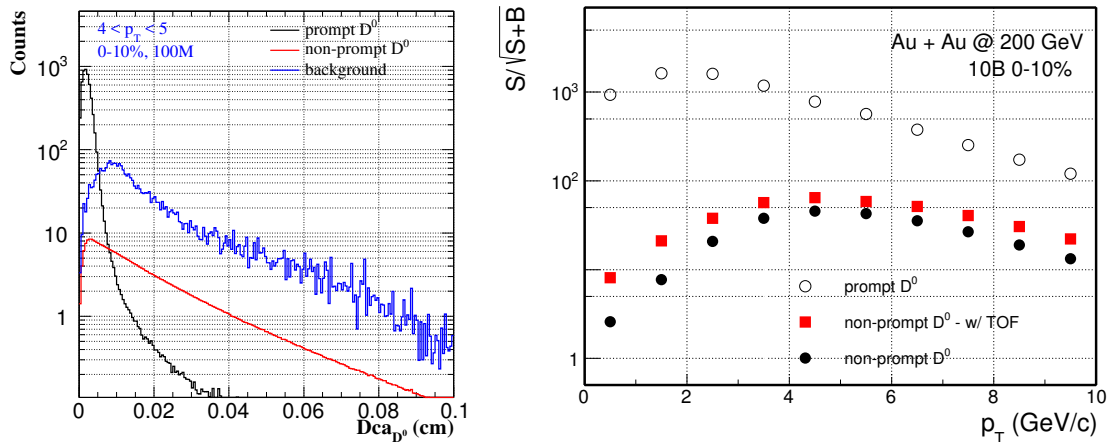


Figure 11: (Left) Simulated D^0 DCA distributions for prompt (black), non-prompt (red) as well as background (blue) contributions for 100M 0-10% central Au+Au events. (Right) Estimated prompt and non-prompt D^0 significance as a function of p_T for 10 billion 0-10% central Au+Au collisions at $\sqrt{s_{NN}} = 200$ GeV with sPHENIX MVTX detector. The red squares represent the estimated significance for non-prompt D^0 with a TOF detector for particle identification.

5.3 Event pileup effects

399

400 With the projected high RHIC beam luminosity, a collision rate up to 2 MHz (100 kHz) is expected
 401 for $p+p$ (Au+Au) collisions in sPHENIX. Since the integration time of the MVTX MAPS chip is about
 402 $4 \mu s$ (corresponding to 37 beam crossings), a pile-up of hits from multiple collisions during this detector
 403 electronics integration time window is expected for each triggered event. Based on the above numbers, on
 404 average, about 8 (0.4) pile-up events in $p+p$ (Au+Au) collisions are expected per triggered event. In addi-
 405 tion, less than 50% of the pile-up events will be located inside the Z-vertex range of the MVTX acceptance,
 406 $|Z_{Vertex}| < 10$ cm, because the collisions are widely distributed along z -axis ($\sigma_z \sim 40$ cm). A preliminary
 407 study shows that these pile-up events in $p+p$ collisions can be easily distinguished from the hard scattering
 408 physics event of interest within the MVTX acceptance over $|Z_{Vertex}| < 10$ cm, where the primary vertex
 409 can be reconstructed and well separated from others with a resolution of $\sim 20 \mu m$. In the case of Au+Au
 410 collisions, the pile up events will increase the overall detector hit occupancy. With the average 0.4 pile-up
 411 events, the occupancy in the innermost layer ($\sim 5 \times 10^7$ channels) will still be very low even in the central
 412 Au+Au collisions (an average of ~ 1500 particles per event). The STAR PXL detector with $186 \mu s$ integra-
 413 tion time observed that the background hit density (including from pileup MB hadronic collisions as well
 414 as ultra-peripheral collisions) to MB signal hit density ratio is about 6:1 at 50 kHz Au+Au collision rate.
 415 With $4 \mu s$ integration time at 100 kHz, we expect the ratio of the background hit density to MB signal hit
 416 density to be about 0.25:1. The MVTX will also provide excellent space point resolution for matching to
 417 the INTT, and to the inner TPC (which has a much longer integration time ($\sim 36 \mu s$)) to further reduce the
 418 combinatorial fake tracks. A GEANT analysis framework is under development to fully simulate the event
 419 pile-up effects on offline track reconstruction, and more detailed studies with a realistic detector response
 420 and physics event simulation will be carried out soon.

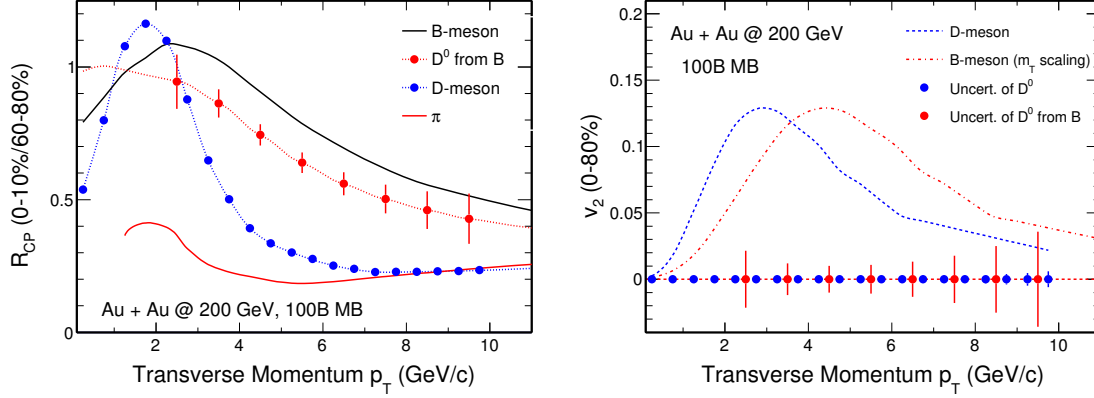


Figure 12: Statistical uncertainty estimation for R_{CP} (left) and v_2 (right) of non-prompt D^0 measurements from 100 billion Au+Au 200 GeV events. In the left plot, the D -meson and B -meson curves are based on calculations from Duke, TAMU and CUJET groups for 0-10% R_{AA} [5, 21, 22], and the dashed curve represents the non-prompt D^0 from B -meson decays. In the right plot, the D -meson curve is a fit to STAR recent D^0 v_2 data points [6] and the B -meson curve is calculated from the D -meson assuming the m_T scaling. The blue and red data points with the vertical bars indicate the statistical uncertainty projections for both D -meson and non-prompt D^0 (B decays) measurements.

6 Technical Scope and Deliverables

In this session, we summarize the technical scope and deliverables of the proposed MVTX project.

6.1 MAPS chips and stave production

We have reached an agreement with the ALICE ITS Upgrade Project management to produce the needed ~ 1000 ALPIDE MAPS chips for the sPHENIX MVTX upgrade. These chips will be produced by Tower Jazz as part of the ALICE ITS upgrade project. The complete QA of the produced MAPS chips will be carried out by the Korean collaborators led by Yonsei University. sPHENIX stave mechanical carbon frames and connectors, which are identical to the ALICE ITS Upgrade Inner Barrel detectors, will be fabricated and tested using the ALICE ITS Upgrade facilities at CERN. The sPHENIX collaboration will provide additional manpower, including students, postdocs and technicians, to help the stave assembly, mechanical survey and full stave readout test in the CERN ITS/IB upgrade labs. The sPHENIX project will eventually obtain 68 fully tested staves from ALICE (which includes 20 spares) and assemble the final detector in the U.S., using the existing facilities at LBNL used for the ALICE ITS mid-layer upgrade project.

6.2 Readout integration and testing

The MVTX readout electronics interfaces the MAPS staves and the sPHENIX DAQ, and also the trigger and slow control systems that monitor and record the status of MAPS chips. There are 48 staves in total (12/16/20 staves for layer 0/1/2, respectively). One Readout Unit (RU) is connected to one stave that contains 9 independent MAPS chips through 9 high-speed copper links. Each link is a point-to-point connection between RU and one MAPS chip, capable of data transmission speed 1.2 Gb/s. A total of 48 RUs are located about 5m away from the MVTX detector, in special 6U VME crates; the exact location of these crates is to be determined later. Data collected by RUs will be sent out through optical fibers to the Common Readout Units (CRU) in the sPHENIX Counting House (CH). The current readout plan is to use the ALICE RU for the stave readout, and modify the ALICE CRU firmware to reformat the data according to the sPHENIX specifications. The R&D effort of the MVTX-sPHENIX readout integration will be carried out by the LANL LDRD project. Figure 13) shows the readout chain of the MVTX system in sPHENIX.

To mitigate potential technical and schedule risks in the ALICE CRU development, we are also exploring

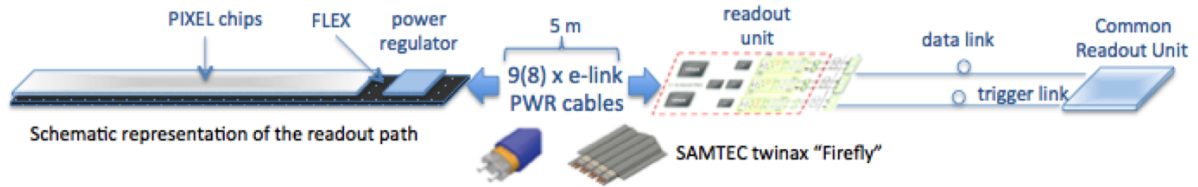


Figure 13: MVTX readout chain in sPHENIX. Readout Units are located about 5m from the MVTX, MAPS data are sent from RUs to CRUs in the Counting House through high-speed fiber optic links.

447 other options to integrate the MVTX readout into the sPHENIX DAQ system. An interesting alternative
 448 DAQ back-end option to CRU is the FELIX PCIe card [23], which is designed as a high-throughput interface
 449 card with front-end and trigger electronics in the ATLAS Upgrade framework and is also considered as an
 450 option for sPHENIX TPC readout. The FELIX PCIe card provides comparable specifications to the CRU,
 451 including 48-bidirectional GBT link to front-end, PCIe16-Gen3 interface to the hosting server for data
 452 output, and a large Xilinx 7-Series Kintex Ultrascale FPGA. The prototype FELIX card is available for
 453 testing and a production system is planned to be delivered to the ATLAS phase-I upgrade at the end of 2018,
 454 which also matches the R&D and production need for the sPHENIX MVTX detector.

455 6.3 Mechanical carbon structures

456 A description of the carbon fiber mechanical structures for the sPHENIX MVTX detector is provided in
 457 this chapter. The mechanical structures developed for the ALICE ITS Upgrade Inner Barrel are compatible
 458 with the general sPHENIX detector infrastructure and constraints with small modifications. In this proposal,
 459 the ITS Upgrade mechanics design will be used as the baseline for the sPHENIX MVTX detector mechanics.
 460 The design will be reviewed and adapted at LANL. The detector and service support carbon fiber structures
 461 will be fabricated at LBNL.

462 After discussing the requirements in Sec. 6.3.1, the mechanical structure that supports the staves in
 463 layers is illustrated in Sec. 6.3.2, while Sec. 6.3.3 describes the cable routing to the staves through the
 464 service barrels.

465 6.3.1 General requirements

466 The layout of the sPHENIX MVTX detector mechanical structure has been developed to fulfill the
 467 following design criteria:

- 468 • minimize material in the sensitive region;
- 469 • ensure high accuracy in the relative position of the detector sensors;
- 470 • provide an accurate position of the detector with respect to the TPC and the beam pipe;
- 471 • locate the first detector layer at a minimum distance to the beam pipe wall;
- 472 • ensure structure thermo-mechanical stability in time;
- 473 • facilitate accessibility for maintenance and inspection;
- 474 • facilitate assembly and disassembly of the detector layers and staves.

475 The main mechanical support structure of the sPHENIX MVTX detector has the shape of a barrel. It
 476 holds in position the three detector layers. The barrel is divided into two halves, top and bottom, which are

477 mounted separately around the beam pipe. The barrel is composed of a detector section and a service section.
 478 The staves are housed in the detector barrel and are connected via electrical signal connections and power
 479 cables to patch panels. The patch panels are located immediately outside of the TPC. The service barrel
 480 integrates the cable trays that support the signal and power cables through their routes from the detector
 481 staves to the patch panels. Pipes that connect the vertex on-detector cooling system to the cooling plant in
 482 the sPHENIX hall are also routed through the service barrels.

483 6.3.2 Detector support structure

484 The main structural components of the detector barrels are the end-wheels and the Cylindrical and
 485 Conical Structural Shells (CCSS).

486 The end-wheels, which are light composite end-rings, ensure the precise positioning of the staves in a
 487 layer. They provide the reference plane for fixing the two extremities of each stave. Staves are positioned
 488 on the reference plane by two connectors that engage a locating pin fixed in the end-wheels at both ends.
 489 The stave position is then frozen by a bolt that passes through the end-wheels and is screwed inside the
 490 connectors. This system ensures accurate positioning, within 10 μ m, during the assembly and provides the
 491 possibility to dismount and reposition the stave with the same accuracy in case of maintenance. The end-
 492 wheels on the front side also provide the feed-through for the services. The different layers are connected
 493 together to form the barrel. An outer cylindrical structural shell (CYSS) connects the opposite end-wheels
 of the barrel and avoids that external loads are transferred directly to the staves (see Figure 14). In order

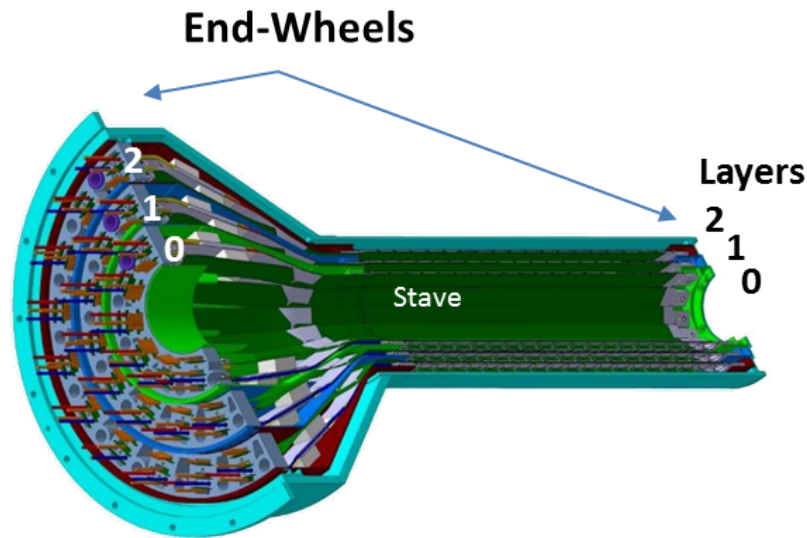
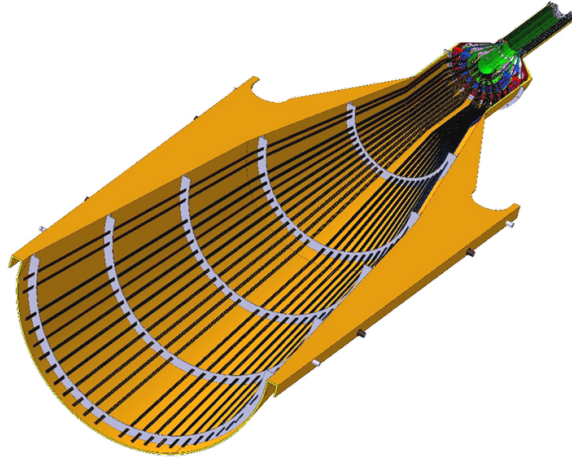


Figure 14: MVTX Half-Barrel, with the three half-layers fixed to the end-wheels. The layout shown here is based on the ALICE ITS Upgrade Inner Barrel design.

494 to minimize the material budget in the detection area and to facilitate installation and removal, the barrel is
 495 conceived as a cantilever structure supported at one end. A full scale prototype has been developed to verify
 496 the production process and the assembly procedure.
 497

498 6.3.3 Service support structure

499 The service support structure design will be adapted from the ITS Upgrade Conical Support Shell
 500 (COSS) (see Figure 15) to match the sPHENIX TPC and general detector dimensions. The services at-
 501 tached to the detector barrel must be inserted or retracted together with the detectors. All services, including



Service Half Barrel

Figure 15: Conical Support Shell (COSS) forming the service half-barrel. The service barrel is an extension of the detector barrel and integrates all services, including cooling pipes, power, and signal cables. The layout shown here is based on the ALICE ITS Upgrade Inner Barrel design. It will be adapted to match the sPHENIX TPC and general detector dimensions.

502 cooling pipes, power, and signal cables, will be integrated into the service barrel, which is an extension of
 503 the detector barrel. Power cables will be grouped with the cooling tubes in the service barrel in order to
 504 remove the heat they generate. The services layout will follow the detector modularity. The services will
 505 be grouped per detector half-barrel and routed from the detector to a patch panel located in an accessible
 506 area outside the TPC on the TPC service support wheels. Inside the TPC, the service barrels will form a
 507 half-cone, jutting from the MAPS detector to the TPC service support wheel. The assembly composed of
 508 half detector barrel and half service barrel is inserted or extracted from the TPC bore by means of two sets
 509 of lateral rollers fixed on the barrels and sliding on their corresponding rails provided by the cage. The ser-
 510 vice barrel itself is a light composite structure that has to provide both structural stiffness and dimensional
 511 stability, to guarantee a precise installation of the sPHENIX MVTX detector inside the TPC.

512 **6.4 Mechanical integration**

513 MIT will be working on the integration of MVTX vertex detector into the current sPHENIX detector at
 514 BNL, working closely with the other detector groups. The support system designed in the ALICE version
 515 of this detector is cantilevered but this constraint doesn't exist in the sPHENIX design. This gives MIT
 516 flexibility in design of the new support system for the MVTX. The geometry of sPHENIX will also require
 517 a new design for the services wheel which in principle can also be part of the support system. The service
 518 wheel will have to accommodate support and organization of the power and signal cables as well as the
 519 cooling tubes for each stave. There will also have to be accommodations for positioning and alignment of
 520 the detector as well as adequate fiducialization to allow for final survey. The current design of the detector
 521 includes air cooling of some components, which will also have to be incorporated into the design of the end
 522 wheels. MIT will work with the carbon fiber group at Berkeley as well as the group at CERN producing
 523 the staves to accomplish all of these goals. An extensive testing plan will need to be put in place to ensure
 524 that the final assembly will function as required. MIT will also work closely with the sPHENIX BBC Min
 525 Bias Trigger and INTT Tracking groups to ensure that choices made early in the design cycle will integrate
 526 smoothly with their detectors and systems in the spectrometer.

527 MIT will lead the design in the cooling system for the staves. The current thought is to use a sub-
 528 atmospheric water system. This will be similar to the system designed for the ALICE MAPS Vertex Tracker,
 529 adapted for the sPHENIX MVTX configuration. This design is being considered such that for any unfore-
 530 seen leak develops in the system, water doesn't drip onto the other detectors and damage them, as sPHENIX
 531 has multiple barrel detectors. MIT will use CFD analysis to ensure that the cooling system will be adequate
 532 for the staves. Figure 16 shows the proposed integrated mechanical support system of the MVTX, adopted
 from ALICE ITS upgrade design.

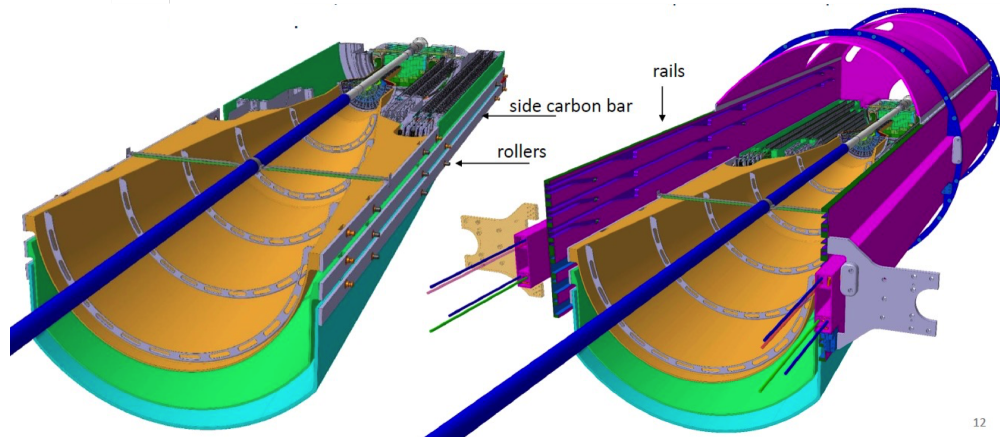


Figure 16: Basic structure of the the sPHENIX MAPS Vertex Detector mechanical supporting system.

533

534 6.5 Power System

535 The power system for the sPHENIX MVTX is included in the scope of participation of LBNL. LBNL
 536 is currently developing the power system for the ALICE ITS Upgrade. The prototypes are being currently
 537 tested and the production boards are being designed. The system meets the current sPHENIX MVTX
 538 detector requirements and its flexible design can be easily adapted to further needs. A brief description of
 539 requirements, architecture and main components is reported in this chapter.

540 6.5.1 Power system requirements

541 The requirements for the powering system (PS) are closely inter-dependent with the sensor and module
 542 FPC requirements, and with the detector environmental and operating conditions. These are most succinctly
 543 expressed as:

- 544 • Supply power (sensor supply and bias) to the staves such that:
 - 545 – Module sensor efficiency $\geq 99\%$
 - 546 – Module sensor noise rate $< 10^{-6}$
- 547 • Tolerate the radiation environment at the power board location.
- 548 • Interface to the RDO board for control of PS functions and readout of parameters.
- 549 • Fit into the space allocated in the vertex detector integration envelopes.

550 This design will be tested in the development of the staves for the ALICE ITS Upgrade and optimized
 551 for sPHENIX. The desirable functional attributes for system include:

- 552 • Overcurrent protection for each power channel
- 553 • Remote current readout for each power channel
- 554 • Remote voltage readout for each power channel
- 555 • Remote voltage setting capability for each channel

556 These attributes will allow for the protection of the sensors from damage due to latch-up conditions and,
 557 should there be any damage that increases current draw, to adjust the voltage to bring the sensors back into
 558 the operating voltage envelope.

559 6.5.2 Power system architecture

The structure of the power system is shown schematically in Figure 17. In this diagram, the main power

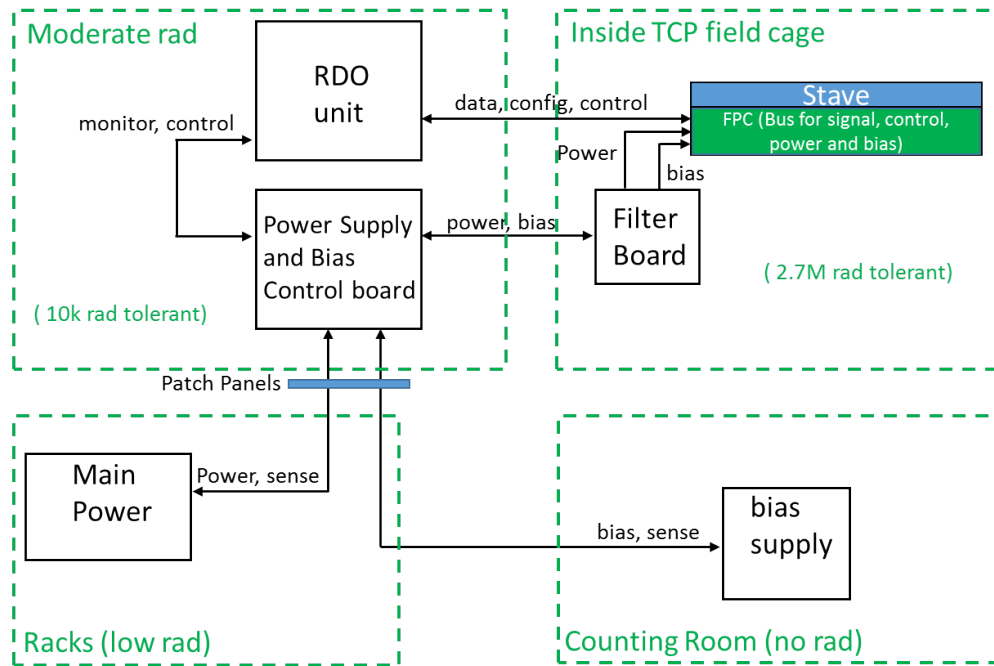


Figure 17: Basic Structure of the sPHENIX MVTX Vertex detector power system. Note the expected radiation load for each architecture block

560 supplies are expected to be located in low-radiation environment, tens of meters far from the interaction
 561 point. The main power supplies are expected to be CAEN mainframes populated with A3009/A3009HPB
 562 radiation tolerant CAEN power modules located in the racks in the hall. The back bias power supplies are
 563 expected to be CAEN mainframes populated with A2518 CAEN power modules located in the sPHENIX
 564 Counting House. All other boards shown are custom designs. The power supply and control board (PSCB)
 565 are being developed for the ALICE ITS Upgrade. They will contain the radiation tolerant power regulators,
 566 shunt resistors, overcurrent protection circuitry, current and voltage measuring circuitry and remote voltage
 567 setting circuitry. This set of boards will be located adjacent to the RDO crates at a larger radial distance and
 568 in a lower radiation. The primary function of the filter boards is to provide sufficient capacitive filtering to
 569 provide a well-regulated supply voltage to the power bus and sensor modules. This architecture is shown in
 570 Figure 18).

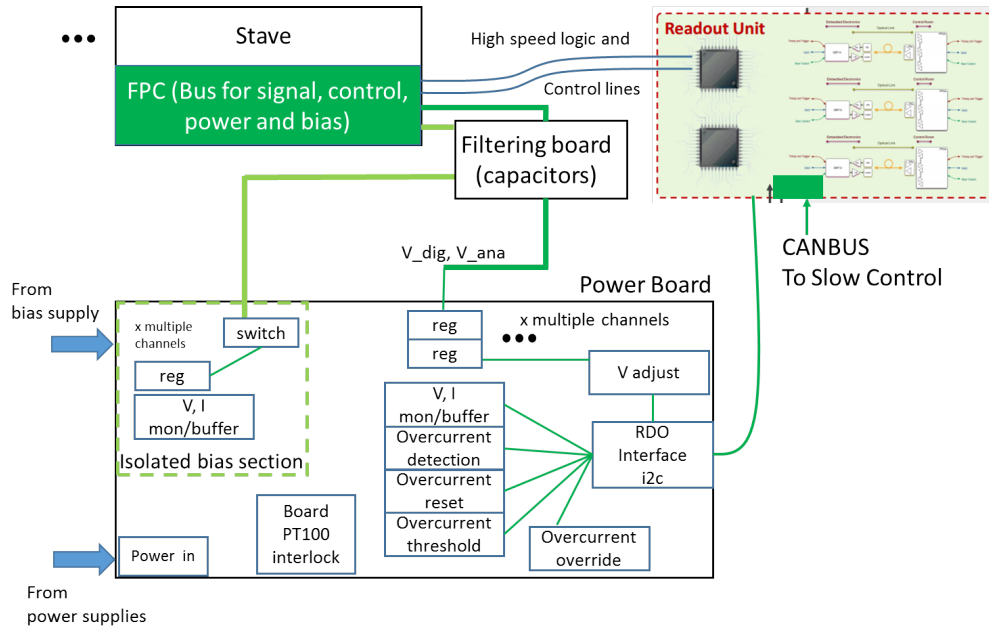


Figure 18: Basic architecture of the power board

6.6 MAPS stave assembly and testing at CERN

Following the completion of the ALICE ITS/IB assembly, experienced CERN techs will continue working on stave assembly for the sPHENIX MVTX project, using the same automated chip mounting machines at ALICE ITS/IB assembly labs. Students and postdocs from sPHENIX collaboration will work with CERN techs to perform the QA of the assembled staves, including visual inspection, test the stave readout at full speed on the test bench, analyze test data to quantify the quality and performance of the staves and produce QA traveler for each stave. Fully tested staves will be sent to LBNL to make half barrel detectors.

6.7 Detector assembly

The scope of participation of LBNL in the sPHENIX MVTX detector includes also the assembly of the staves into the half detector support structure. The three layers, starting from the innermost one, consist of 12, 16 and 20 staves, respectively. Each stave is approximately 29 cm in length and contains nine Pixel Chips in a row connected to the FPC, which embeds signal, control, power and bias lines. The staves will be fabricated at CERN, as described in Sec. 6.6, and shipped to LBNL. The assembly scope of work will consist of:

1. Inspection, functional testing and validation of received staves
2. Metrology survey of the staves
3. Mounting of the staves onto the end-wheels to form the layers
4. Functional testing and validation of the layers
5. Metrology survey on the layers
6. Assembly of the three layers together and to the cylindrical support into the half detector

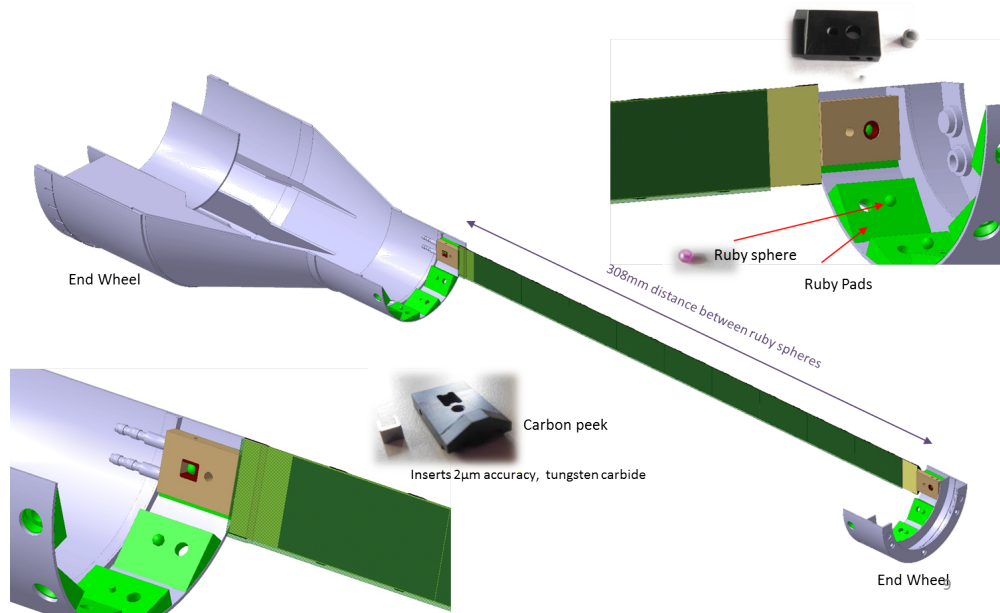


Figure 19: Stave assembly into layer

- 592 7. Functional testing and validation of the assemblies
- 593 8. Metrology survey on the final assemblies
- 594 9. Packing and shipment of the final assemblies to BNL.

595 The testing system is being developed by the ALICE Collaboration and is based on the ALICE RDO sys-
 596 tem. After the initial test, the stave is positioned on the end wheels reference planes by connectors at both
 597 extremities that engage a ruby sphere fixed in the reference plane (see Figure 19). The stave position is then
 598 fixed by a bolt. The front side end-wheel includes the service barrel conical extension to hold and route all
 599 services, including cooling pipes, power, and signal cables. The three layers are assembled together and to
 600 the half detector CYSS, and the relative position is achieved by reference pins (see Figure 20). After each
 601 assembly step the assemblies are tested for validation and reworked if necessary, and a metrology survey is
 602 performed. The half detectors are finally ready to be packed and shipped to BNL.

603 **6.8 Online software and Trigger**

604 The online software for the MVTX will be part of the sPHENIX data acquisition (DAQ). The sPHENIX
 605 DAQ closely follows the design of the PHENIX DAQ [24]. The architecture is a fully pipelined design,
 606 which allows the next event to be triggered without waiting for the previous event to be fully processed.
 607 The existing PHENIX design allows for a depth of 4 such events to be buffered in front end modules before
 608 transmission. This multi-event buffering is the key concept to achieve the design event rate of 15 kHz while
 609 preserving livetime.

610 Figure 21 shows a schematic overview of the trigger, the front-end and the back-end systems. The Global
 611 Level 1 (GL1) system provides the trigger to the Master Timing Module (MTM), which is then distributed
 612 to the Granule Timing Modules (GTM). These GTMs provide the subsystem-specific trigger signals and

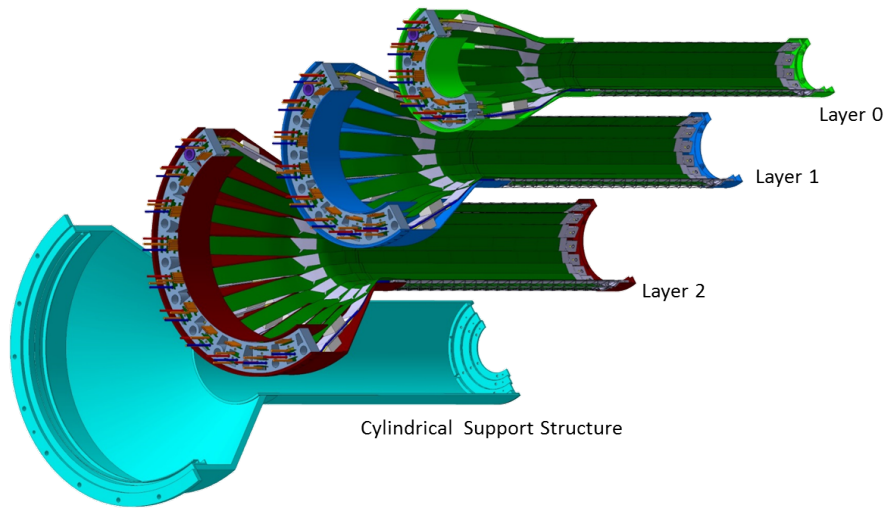


Figure 20: Layer assembly into half detector

613 timing to the MVTX Front End Modules (FEM). The data selected by the trigger system flow from the
 614 FEMs to Data Collection Modules (DCMs). Only the latest generation of the data collection module, the
 615 DCM-II, will be used. The DCM-II, which were developed for the PHENIX silicon vertex detectors, run
 616 detector-specific FPGA code to zero-suppress and package the data. This provides the freedom to change
 617 the data format as necessary by loading a new version of the FPGA code. A DCM-II has inputs for 8 data
 fibers. A group of DCM-II's interface with the commodity computers called Sub-Event Buffers (SEBs) via

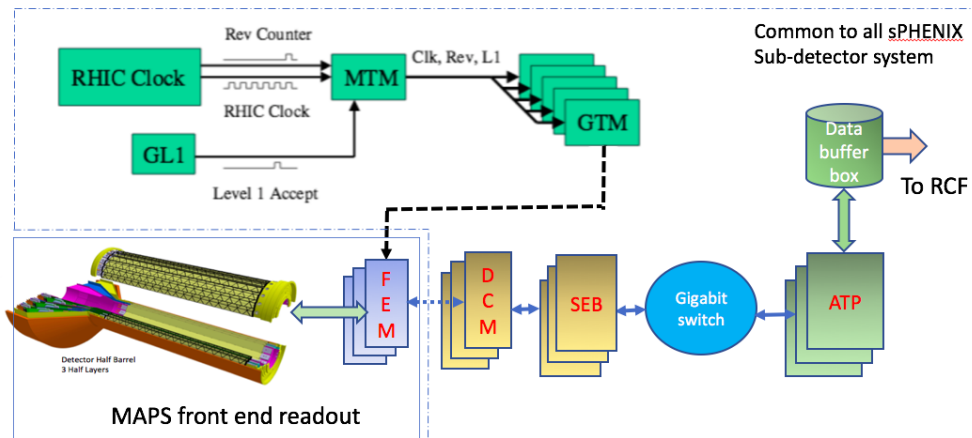


Figure 21: Online readout architecture for MAPS.

618
 619 1.6 GBit/s serial optical links through a custom PCIe interface card, the JSEB-II. Due to overhead in the
 620 data encoding, the effective bandwidth through the fiber is 1.28 GBit/s. This 4-lane PCIe card is capable of
 621 sustaining 500 MB/s input into the SEB. This bandwidth is needed to achieve the envisioned event rate of
 622 about 15kHz. Each SEB only holds a fragment of the data of a given collision, which have to be combined
 623 together with data fragments from other sPHENIX detectors into a full event. This is accomplished on

624 computers called Assembly and Trigger Processors (ATPs) as shown in Fig. 21.

625 Other options could include the adaptation of the LHCb/ALICE CRU or ATLAS FELIX as shown in 22,
 as proposed for the sPHENIX TPC readout.

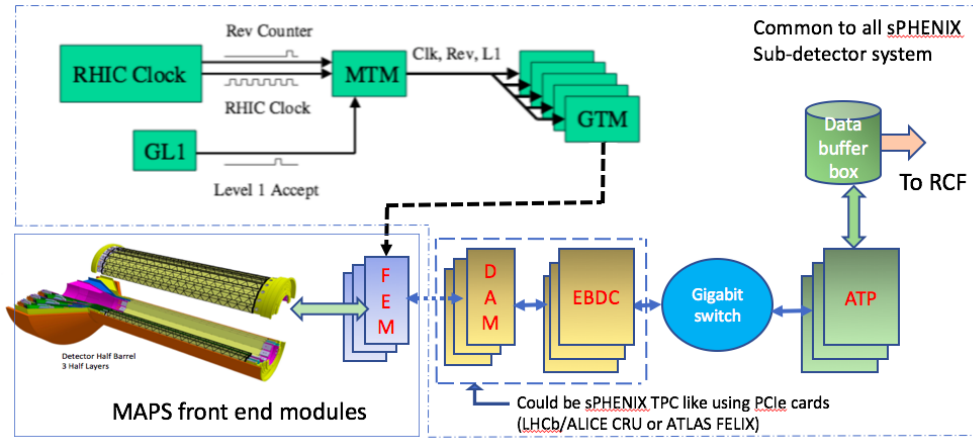


Figure 22: Online readout architecture for MAPS using PCIe cards.

626

627 6.9 Offline software - detector simulation, geometry, offline tracking

628 In sPHENIX, tracking simulation and reconstruction is performed in a global software framework including all tracking subsystems, inner pixel vertex detector (MVTX), intermediate silicon strip detector (INTT) and the outer time projection chamber (TPC).

- 631 • The sPHENIX software framework provide a custom-designed unified platform for detector simulation, raw data decoding, reconstruction and analysis. It has been successfully used in data analysis and simulation for the PHENIX collaboration in the past decade.
- 632
- 633
- 634 • The GEANT4 simulation toolkit [25] is employed to simulate interaction between collision product and full sPHENIX detector package and MVTX. MVTX group has provided the detailed geometry description of the sensitive and passive materials of the detector system. The hit information from GEANT4 is digitized into detector hit.
- 635
- 636
- 637
- 638 • Adjacent hits in the MVTX is grouped into a single cluster. We employ a 5-dimensional Hough transform to locate the helical hit patterns from tracks bending through the solenoid field.
- 639
- 640 • Clusters belong to the same track are fit via a Kalman-filter-based generic track-fitting toolkit, GenFit2 [26], to extract track parameter of displacement at vertex and momentum vector at vertex.
- 641
- 642 • All tracks are fed into a generic tracking fitting toolkit, RAVE [27], to determine the locations of the primary and secondary vertexes.
- 643

644 The track and vertex information is available for offline analysis through the sPHENIX software framework, which has been used to produce the preliminary performance plots discussed in Section. 5. This software framework will be further developed for physics and detector simulations and eventually for physics data analysis using the MVTX detector.

647

648 **7 Organization and Collaboration**

649 Here we discuss the current collaborating institutions and their focus areas. Based on their technical
650 expertise and available resources, LANL, LBNL and MIT/Bates groups are leading the three major technical
651 tasks of the project: 1) readout electronics integration; 2) carbon mechanical support frames production and
652 3) cooling and mechanical system integration, respectively.

653 **Los Alamos National Lab (LANL)** : Readout electronics and mechanics integration.

654 **Lawrence Berkeley National Lab (LBNL)** : Carbon structure, production, LV and HV power system, full
655 detector assembly and test.

656 **Brookhaven National Lab (BNL)** : System integration and services, safety and monitoring.

657 **Massachusetts Institute of Technology (MIT/Bates)** : Mechanical system integration and cooling.

658 **Massachusetts Institute of Technology (MIT)** : Stave assembly and testing at CERN.

659 **University of Texas at Austin (UT Austin)** : MVTX readout electronics integration and testing.

660 **University of Colorado** : *b*-jet simulations and future hardware.

661 **Iowa State University (ISU)** : Detector assembly and testing, simulations.

662 **Florida State University (FSU)** : Offline and simulations.

663 **University of New Mexico (UNM)** : LV cabling & connectors.

664 **New Mexico State University (NMSU)** : Tracking algorithm and physics simulations.

665 **Georgia State University (GSU)** : Online software and trigger development.

666 **University of California at Los Angeles (UCLA)** : Simulation and readout testing.

667 **University of California at Riverside (UCR)** : Detector assembly and testing, simulations.

668 **Yonsei University (Korea)** : MAPS chips QA and readout, simulations

669 **RIKEN/RBRC (Japan)** : Mechanical integration, cooling, cabling, simulation, patten recognition.

670 **Purdue**: Detector assembly and testing, analysis. Silicon lab available.

671 **Central China Normal University (CCNU/China)**: MAPS chip and stave test at CERN and/or CCNU.

672 **Univ. of Science and Technology of China (USTC/China)**: MAPS chip and stave test, simulations.

673 Figure 23 shows the organization chart and tasks assigned for each Institution.

674 Detector R&D is underway at Los Alamos National Lab utilizing the internal LDRD funding (\$5M
675 over 3 years, FY17-19). This R&D aims to develop a prototype telescope detector with four MAPS staves
676 and the full readout electronics chain needed to comply with the sPHENIX DAQ. LANL will work closely
677 with ALICE ITS Upgrade Group at CERN, UT-Austin, LBNL and BNL groups on the final MVXT read-
678 out system design and production. The LANL LDRD project will also carry out the initial design of the
679 MVTX mechanical system to integrate into the sPHENIX. MIT Bates Center will lead the final mechanical

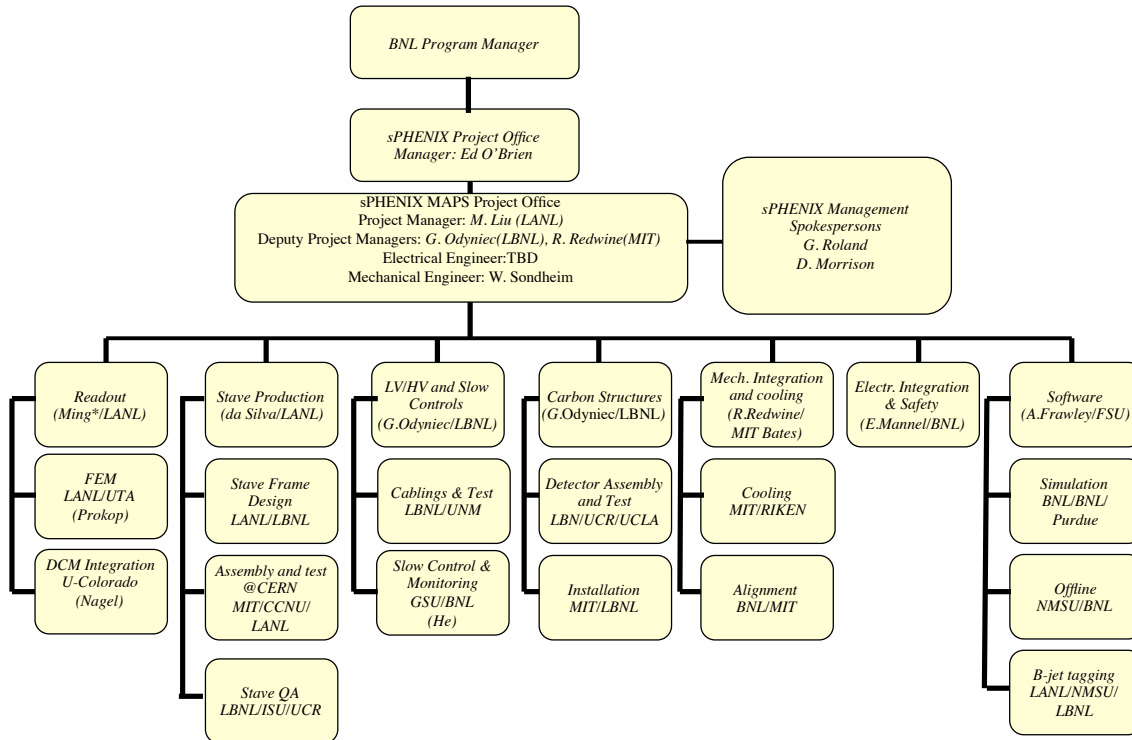


Figure 23: Organization chart of the MVTX project.

680 integration effort and has designated 0.25 FTE for an engineer and 1 FTE for a technician to work on the
 681 mechanical system integration. LBNL will lead the effort of carbon structure fabrication, detector assembly
 682 and system readout test, and also the production of the LV and HV power distribution boards and control
 683 system based on the ALICE design. Other institutions will lead or help on various key tasks according to
 684 their available resources and expertise, as shown in Figure 23.

685 8 Schedule and Cost Baseline

686 The MVTX project for sPHENIX relies on the fact that much of the conceptual design, prototype design,
 687 and prototyping has/will be done by the ALICE group at CERN and through a Los Alamos National Labora-
 688 tory LDRD(Laboratory Directed research and Development) development effort. The cost and schedule for
 689 the is proposed for DOE/BNL support consists of final design efforts, procurement, assembly and installa-
 690 tion. Presented here will be the proposed effort for the DOE/BNL portion. The complete cost and schedule
 691 file including the ALICE and LDRD effort is found in the appendix. The total project cost is \$4.9M after
 692 ~ 30% contingency applied. Projected finish date is the 4th Quarter of 2021.

693 8.1 Schedule

694 Figure 24 is a high level view of the Cost and Schedule Gantt chart showing ALICE milestones that
 695 constrain the scheduling of the MVTX effort. The MVTX start date for the start of the technical design is
 696 in the 1st quarter of FY 2018, start construction is in the 4th quarter of FY 2018, installation and ready for

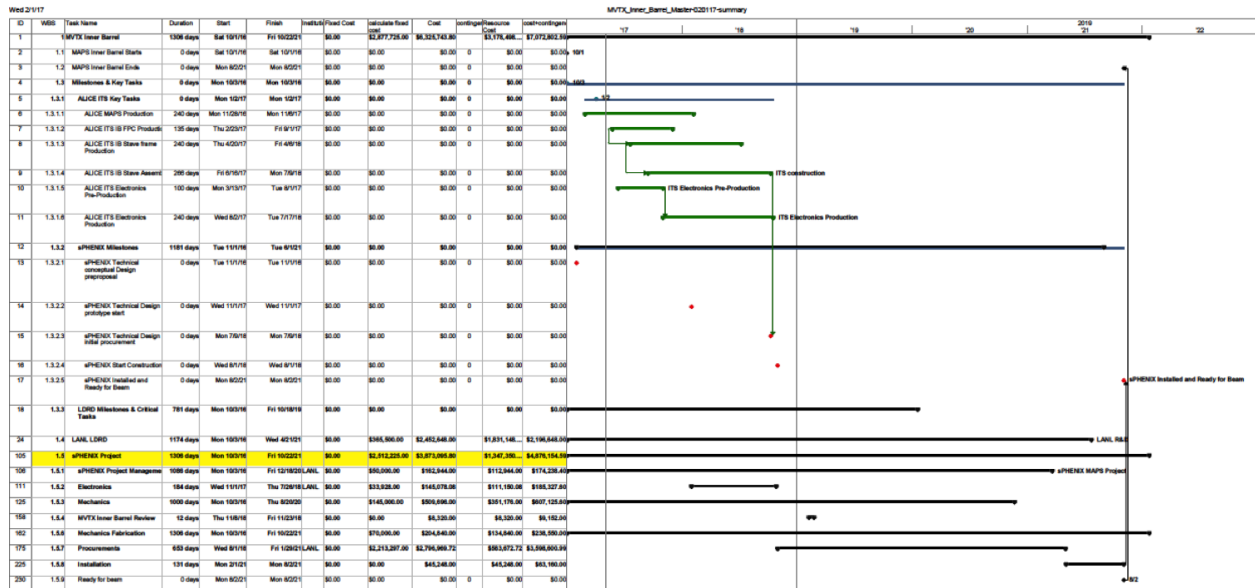


Figure 24: MVTX High Level Cost and Schedule.

697 beam is in the 3rd quarter of FY 2021.

698 An important constraint on this schedule is the production activities at ALICE. To reduce the MVTX
 699 project cost it is important that we are able to take advantage of the production lines at CERN. The Cost
 700 and Schedule is designed to use the CERN personnel and production lines at CERN. By doing this MVTX
 701 project does not have to implement a completely new production facility in the US with the necessary
 702 equipment, clean facilities, jigs, infrastructure, and personnel training that would be necessary. Currently,
 703 the end of ALICE production is in the 3rd quarter of FY 2018. Negotiations with CERN/BNL will be needed
 704 to accomplish the beginning of MAPS stave production at that time.

705 8.2 Cost

706 The cost of items in the Cost and Schedule are derived from actual ALICE costs and scaled by the
 707 number of staves. Since in the stave production cost at CERN, labor costs are not included, we have included
 708 a separate task under procurements to provide for our use of the CERN personnel in producing our staves.
 709 Electronics costs are based on obtaining Gerber files from ALICE and fabricating them in the US. This
 710 was done previously for the mini-CAPTAIN LANL LDRD with great success. Costs were based on the
 711 board complexity and applied to the MVTX electronics. The cost of the common readout board which will
 712 be designed at LANL is based on a similarly complex board that was recently fabricated for the FVTX
 713 detector at PHENIX. Mechanical procurements costs are based on ALICE procurements of the same item.
 714 The mechanical design of the MVTX detector will be a replication of the ALICE design but since the
 715 MVTX detector will sit inside the Intermediate Tracker which is not yet designed we have included a 50%
 716 contingency to cover a possible redesign. Mechanical Integration into sPHENIX requires a clear definition
 717 of the surrounding systems. Unfortunately, because the inner volume is still in a state of flux, we have
 718 looked at the global support structure for the TPC as an estimate for our needs but with a large contingency.
 719 Contingency is risked based and varies between 25% and 50%.

720 **8.3 Resources**

721 The level of resources is based on previous experience in other projects such as FVTX/PHENIX upgrade,
722 ALICE/ITS upgrade, and the recent HFT/STAR upgrade. Resource costs are institution specific with fully
723 costed hourly rates used.

724 **8.4 Milestones**

725 Here we show the milestones of the project.

| Milestones | Time |
|-------------------------|-----------------|
| MVTX Preproposal finish | 4th Qtr FY 2017 |
| MVTX Proposal Review | 2nd Qtr FY 2018 |
| Stave Procurement | 4th Qtr FY 2018 |
| Start Construction | 4th Qtr FY 2018 |
| Installation | 1st Qtr FY 2021 |
| Ready for Beam | 4th Qtr FY 2021 |

Table 3: Milestones

726 **8.5 Major Cost Items**

727 Here we list the cost of major items.

| WBS | Task Name | Cost (K) | Cost with Contingency (K) |
|------------|---------------------------|-----------------|----------------------------------|
| 1.5.7.1.1 | Produce 68 staves | \$650 | \$880 |
| 1.5.7.1.2 | CERN Manpower | \$500 | \$680 |
| 1.5.7.2.1 | Readout Units(RDO) | \$290 | \$360 |
| 1.5.7.2.2 | Optical Links | \$83 | \$100 |
| 1.5.7.2.3 | Common Readout Units(CRU) | \$180 | \$230 |
| 1.5.7.2.4 | CRU Contingency | \$90 | \$110 |
| 1.5.7.2.16 | Service Half Barrels | \$120 | \$150 |

Table 4: Major Cost Items

728 **End of proposal narrative; supplemental materials to follow.**

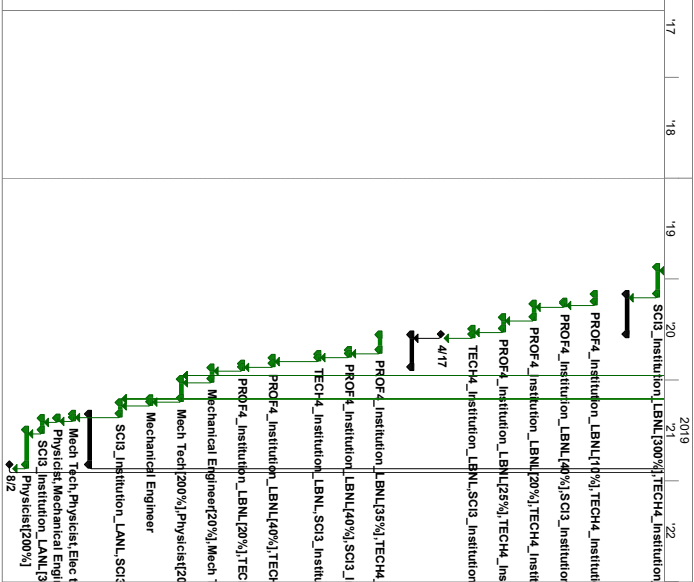
729 **9 Project Timeline, Deliverables, and Tasks**

| ID | WBS | Task Name | Duration | Start | Finish | Instant/Fixed Cost | Calculate fixed cost | Cost | contingent/Resource Cost | cost-contingent |
|-----|-------------|----------------------------------|-----------|--------------|--------------|--------------------|----------------------|----------------|--------------------------|-----------------|
| 1 | 1.1 | 1MWTX Inner Barrel | 1306 days | Sat 1/01/16 | Fri 1/02/21 | \$0.00 | \$2,877,725.00 | \$6,325,743.80 | \$3,172,498... | \$7,072,802.59 |
| 2 | 1.1.1 | MAPS Inner Barrel Starts | 0 days | Sat 1/01/16 | Sat 1/01/16 | \$0.00 | \$0.00 | \$0.00 | \$0.00 | \$0.00 |
| 3 | 1.2 | MAPS Inner Barrel Ends | 0 days | Mon 8/2/21 | Mon 8/2/21 | \$0.00 | \$0.00 | \$0.00 | \$0.00 | \$0.00 |
| 4 | 1.3 | Milestones & Key Tasks | 0 days | Mon 10/3/16 | Mon 10/3/16 | \$0.00 | \$0.00 | \$0.00 | \$0.00 | \$0.00 |
| 5 | 1.3.1 | ALICE ITS Key Tasks | 0 days | Mon 12/1/17 | Mon 12/1/17 | \$0.00 | \$0.00 | \$0.00 | \$0.00 | \$0.00 |
| 6 | 1.3.1.1 | ALICE MAPS Production | 240 days | Mon 11/28/16 | Mon 11/6/17 | \$0.00 | \$0.00 | \$0.00 | \$0.00 | \$0.00 |
| 7 | 1.3.1.2 | ALICE ITS IB FPC Product | 135 days | Thu 2/23/17 | Fri 9/1/17 | \$0.00 | \$0.00 | \$0.00 | \$0.00 | \$0.00 |
| 8 | 1.3.1.3 | ALICE ITS IB Slave Frame | 240 days | Thu 4/20/17 | Fri 4/6/18 | \$0.00 | \$0.00 | \$0.00 | \$0.00 | \$0.00 |
| 9 | 1.3.1.4 | ALICE ITS IB Slave Assem | 266 days | Fri 6/16/17 | Mon 7/9/18 | \$0.00 | \$0.00 | \$0.00 | \$0.00 | \$0.00 |
| 10 | 1.3.1.5 | ALICE ITS Electronics | 100 days | Mon 3/13/17 | Tue 8/1/17 | \$0.00 | \$0.00 | \$0.00 | \$0.00 | \$0.00 |
| 11 | 1.3.1.6 | ALICE ITS Electronics | 240 days | Wed 8/2/17 | Tue 7/17/18 | \$0.00 | \$0.00 | \$0.00 | \$0.00 | \$0.00 |
| 12 | 1.3.2 | SPHENIX Milestones | 1181 days | Tue 1/11/16 | Tue 6/11/21 | \$0.00 | \$0.00 | \$0.00 | \$0.00 | \$0.00 |
| 13 | 1.3.2.1 | SPHENIX Technical proposal | 0 days | Tue 1/11/16 | Tue 1/11/16 | \$0.00 | \$0.00 | \$0.00 | \$0.00 | \$0.00 |
| 14 | 1.3.2.2 | SPHENIX Technical Design | 0 days | Wed 11/11/17 | Wed 11/11/17 | \$0.00 | \$0.00 | \$0.00 | \$0.00 | \$0.00 |
| 15 | 1.3.2.3 | SPHENIX Technical Design | 0 days | Mon 7/9/18 | Mon 7/9/18 | \$0.00 | \$0.00 | \$0.00 | \$0.00 | \$0.00 |
| 16 | 1.3.2.4 | SPHENIX Start Construction | 0 days | Wed 8/1/18 | Wed 8/1/18 | \$0.00 | \$0.00 | \$0.00 | \$0.00 | \$0.00 |
| 17 | 1.3.2.9 | SPHENIX Start and Ready for Beam | 0 days | Mon 8/2/21 | Mon 8/2/21 | \$0.00 | \$0.00 | \$0.00 | \$0.00 | \$0.00 |
| 18 | 1.3.3 | LDRD Milestones & Critical Tasks | 781 days | Mon 10/2/16 | Fri 10/18/19 | \$0.00 | \$0.00 | \$0.00 | \$0.00 | \$0.00 |
| 24 | 1.4 | LANL LDRD | 1174 days | Mon 10/2/16 | Wed 4/21/21 | \$0.00 | \$365,509.00 | \$2,482,648.80 | \$1,831,148... | \$2,196,648.00 |
| 105 | 1.5 | SPHENIX Project | 1398 days | Mon 10/2/16 | Fri 10/22/21 | \$0.00 | \$2,312,225.00 | \$3,873,095.80 | \$1,927,350... | \$4,876,454.50 |
| 106 | 1.5.1 | SPHENIX Project Management | 1086 days | Mon 10/2/16 | Fri 12/18/20 | \$0.00 | \$50,000.00 | \$162,944.00 | \$112,944.00 | \$174,428.40 |
| 107 | 1.5.1.1 | Project Manager | 1086 days | Mon 10/2/16 | Fri 12/18/20 | \$0.00 | \$0.00 | \$0.00 | \$0.00 | \$0.00 |
| 108 | 1.5.1.2 | Mechanical Integration | 1086 days | Mon 10/2/16 | Fri 12/18/20 | \$0.00 | \$0.00 | \$56,472.00 | \$56,472.00 | \$62,119.20 |
| 109 | 1.5.1.3 | Electronics Integration | 1086 days | Mon 10/2/16 | Fri 12/18/20 | \$0.00 | \$0.00 | \$56,472.00 | \$56,472.00 | \$62,119.20 |
| 110 | 1.5.1.4 | Travel | 1000 days | Mon 10/3/16 | Thu 8/20/20 | \$50,000.00 | \$50,000.00 | \$50,000.00 | \$0.00 | \$50,000.00 |
| 111 | 1.5.1.4 | Electronics | 184 days | Fri 6/1/18 | Thu 7/26/18 | \$33,928.00 | \$33,928.00 | \$145,078.08 | \$111,150.08 | \$185,327.60 |
| 112 | 1.5.2.1 | Final Electronics Design | 40 days | Fri 6/1/18 | Thu 7/26/18 | \$25,000.00 | \$25,000.00 | \$63,400.00 | \$39,400.00 | \$83,200.00 |
| 113 | 1.5.2.1.1 | Produce RDU first unit | 4 wks | Fri 6/1/18 | Thu 6/28/18 | \$10,000.00 | \$10,000.00 | \$12,400.00 | \$2,400.00 | \$15,500.00 |
| 114 | 1.5.2.1.2 | Test RDU | 2 wks | Fri 6/29/18 | Thu 7/12/18 | \$0.00 | \$0.00 | \$11,200.00 | \$11,200.00 | \$14,000.00 |
| 115 | 1.5.2.1.3 | Produce CRU first unit | 4 wks | Fri 6/1/18 | Thu 6/28/18 | \$15,000.00 | \$15,000.00 | \$17,400.00 | \$2,400.00 | \$23,490.00 |
| 116 | 1.5.2.1.4 | Test CRU | 2 wks | Fri 6/29/18 | Thu 7/12/18 | \$0.00 | \$0.00 | \$11,200.00 | \$11,200.00 | \$15,120.00 |
| 117 | 1.5.2.1.5 | Final Electronics System Test | 2 wks | Fri 7/13/18 | Thu 7/26/18 | \$0.00 | \$0.00 | \$11,200.00 | \$11,200.00 | \$15,120.00 |
| 118 | 1.5.2.2 | MAPS Power System | 82 days | Wed 11/11/17 | Tue 3/6/18 | \$0.00 | \$8,928.00 | \$81,678.08 | \$72,750.08 | \$102,097.60 |
| 119 | 1.5.2.2.1 | Power Boards | 82 days | Wed 11/11/17 | Tue 3/6/18 | \$0.00 | \$8,928.00 | \$81,678.08 | \$72,750.08 | \$102,097.60 |
| 120 | 1.5.2.2.1.1 | Review ALICE PB Design | 20 days | Wed 11/11/17 | Fri 12/11/17 | \$0.00 | \$0.00 | \$26,748.80 | \$26,748.80 | \$33,436.00 |
| 121 | 1.5.2.2.1.2 | Fabricate PB prototype | 30 days | Mon 12/4/17 | Fri 1/19/18 | \$5,771.00 | \$5,771.00 | \$12,883.00 | \$6,912.00 | \$15,863.75 |
| 122 | 1.5.2.2.1.3 | Test PB Prototype | 20 days | Mon 12/27/18 | Fri 2/16/18 | \$1,154.00 | \$1,154.00 | \$24,194.00 | \$23,040.00 | \$30,242.50 |
| 123 | 1.5.2.2.1.4 | Design Production PB | 10 days | Mon 2/19/18 | Fri 3/2/18 | \$2,003.00 | \$2,003.00 | \$15,374.40 | \$13,374.40 | \$19,221.75 |
| 124 | 1.5.2.2.1.5 | Power System Review | 2 days | Mon 3/5/18 | Tue 3/6/18 | \$0.00 | \$0.00 | \$2,674.88 | \$2,674.88 | \$3,343.60 |
| 125 | 1.5.3 | Mechanics | 1000 days | Mon 10/2/16 | Thu 8/20/20 | \$0.00 | \$145,000.00 | \$509,696.00 | \$351,176.00 | \$607,125.60 |
| 126 | 1.5.3.1 | Mechanics Detector Design | 200 days | Wed 11/11/17 | Fri 8/17/18 | \$0.00 | \$23,400.00 | \$23,400.00 | \$218,400.00 | \$310,750.00 |
| 127 | 1.5.3.1.1 | Review ALICE design | 2 wks | Wed 11/11/17 | Wed 11/22/17 | \$0.00 | \$0.00 | \$10,400.00 | \$10,400.00 | \$13,000.00 |
| 128 | 1.5.3.1.2 | modify design if necessary | 5 wks | Thu 11/16/17 | Fri 12/22/17 | \$0.00 | \$0.00 | \$26,000.00 | \$26,000.00 | \$33,800.00 |
| 129 | 1.5.3.1.3 | Modify Service Barrel | 5 wks | Mon 1/1/18 | Fri 2/2/18 | \$0.00 | \$0.00 | \$26,000.00 | \$26,000.00 | \$32,500.00 |

| ID | WBS | Task Name | Duration | Start | Finish | Instant/Fixed Cost | Calculate fixed cost | Cost | config/Resource Cost | cost+config |
|-----|-------------|--|-----------|--------------|--------------|--------------------|----------------------|--------------|----------------------|--------------|
| 130 | 1.5.3.1.4 | design interface to rail system | 5 wks | Mon 2/5/18 | Fr 3/9/18 | \$0.00 | \$0.00 | \$26,000.00 | 25 | \$26,000.00 |
| 131 | 1.5.3.1.5 | Develop MAPS inner tracker mechanical model | 1 mon | Mon 3/12/18 | Fr 4/6/18 | \$0.00 | \$0.00 | \$20,800.00 | 25 | \$20,800.00 |
| 132 | 1.5.3.1.6 | Slave Support Frame & Global Interface to sPHENIX | 168 days | Mon 1/1/18 | Fr 8/7/18 | \$0.00 | \$25,000.00 | \$134,200.00 | 25 | \$109,200.00 |
| 133 | 1.5.3.1.6.1 | Design Interface to sPHENIX | 50 days | Mon 1/1/18 | Fr 3/9/18 | \$0.00 | \$0.00 | \$52,000.00 | .35 | \$52,000.00 |
| 134 | 1.5.3.1.6.2 | FEA Thermal stress analysis | 30 days | Mon 3/12/18 | Fr 4/20/18 | \$0.00 | \$0.00 | \$31,200.00 | .25 | \$31,200.00 |
| 135 | 1.5.3.1.6.3 | prototype test | 60 days | Fr 4/20/18 | Fr 7/13/18 | \$25,000.00 | \$25,000.00 | \$25,000.00 | .25 | \$0.00 |
| 136 | 1.5.3.1.6.4 | final design | 10 days | Mon 7/16/18 | Fr 7/27/18 | \$0.00 | \$0.00 | \$10,400.00 | .25 | \$10,400.00 |
| 137 | 1.5.3.1.6.5 | Mechanics Integration | 15 days | Mon 7/30/18 | Fr 8/17/18 | \$0.00 | \$0.00 | \$15,600.00 | .25 | \$15,600.00 |
| 138 | 1.5.3.2 | Travel MIT | 1000 days | Mon 10/3/16 | Thu 8/20/20 | \$0.00 | \$120,000.00 | \$201,320.00 | 0 | \$81,320.00 |
| 139 | 1.5.3.2.1 | Cooling System | 25 days | Mon 8/20/18 | Fr 9/21/18 | \$0.00 | \$0.00 | \$45,680.00 | .25 | \$45,680.00 |
| 140 | 1.5.3.2.2 | Mock up testing | 10 days | Mon 9/3/18 | Fr 9/24/18 | \$20,000.00 | \$20,000.00 | \$27,200.00 | .25 | \$27,200.00 |
| 141 | 1.5.3.2.2.1 | Final Design of Cooling System | 5 days | Mon 9/17/18 | Fr 9/24/18 | \$0.00 | \$0.00 | \$6,160.00 | .25 | \$6,160.00 |
| 142 | 1.5.3.2.2.2 | Safety Systems review sensors & methods | 40 days | Mon 9/24/18 | Fr 11/6/18 | \$0.00 | \$10,000.00 | \$34,640.00 | .15 | \$6,160.00 |
| 143 | 1.5.3.2.3 | cooling mechanics design | 30 days | Mon 10/8/18 | Fr 11/6/18 | \$10,000.00 | \$10,000.00 | \$28,480.00 | .25 | \$18,480.00 |
| 144 | 1.5.3.2.4 | Slave Assembly Tooling | 40 days | Mon 8/20/18 | Fr 10/9/18 | \$0.00 | \$20,000.00 | \$10,000.00 | .25 | \$10,000.00 |
| 145 | 1.5.3.2.4.1 | design | 20 days | Mon 8/20/18 | Fr 9/7/18 | \$0.00 | \$0.00 | \$20,800.00 | .25 | \$20,800.00 |
| 146 | 1.5.3.2.4.2 | final Jg design | 30 days | Mon 8/20/18 | Fr 10/2/18 | \$0.00 | \$0.00 | \$38,000.00 | .25 | \$38,000.00 |
| 147 | 1.5.3.2.4.3 | Mechanics Final Design Review | 13 days | Mon 10/22/18 | Wed 11/7/18 | \$0.00 | \$0.00 | \$23,376.00 | .25 | \$9,856.00 |
| 148 | 1.5.3.3 | Mechanical design review | 2 days | Mon 10/22/18 | Tue 10/23/18 | \$0.00 | \$0.00 | \$2,464.00 | .10 | \$2,464.00 |
| 149 | 1.5.3.3.1 | Incorporate Review Comments | 10 days | Wed 10/24/18 | Tue 11/6/18 | \$0.00 | \$0.00 | \$6,160.00 | .10 | \$6,160.00 |
| 150 | 1.5.3.3.2 | Complete Final Mechanical Design | 1 day | Wed 11/7/18 | Wed 11/7/18 | \$0.00 | \$0.00 | \$1,232.00 | .10 | \$1,352.00 |
| 151 | 1.5.3.3.3 | Ancillary Systems Metrology design | 40 days | Mon 1/1/18 | Fr 2/23/18 | \$0.00 | \$0.00 | \$41,600.00 | .25 | \$41,600.00 |
| 152 | 1.5.3.4 | Metrology design | 20 days | Mon 1/1/18 | Fr 1/23/18 | \$0.00 | \$0.00 | \$20,800.00 | .25 | \$20,800.00 |
| 153 | 1.5.3.4.1 | Design Jgs | 20 days | Mon 1/29/18 | Fr 2/23/18 | \$0.00 | \$0.00 | \$20,800.00 | .25 | \$20,800.00 |
| 154 | 1.5.3.4.2 | MTVX Inner Barrel Review | 12 days | Thu 1/18/18 | Fr 1/23/18 | \$0.00 | \$0.00 | \$8,320.00 | .10 | \$8,320.00 |
| 155 | 1.5.4 | MTVX Final Design Review | 1 day | Thu 1/18/18 | Thu 1/18/18 | \$0.00 | \$0.00 | \$1,040.00 | .10 | \$1,444.00 |
| 156 | 1.5.4.1 | Incorporate Review Comments | 10 days | Fr 1/19/18 | Thu 1/22/18 | \$0.00 | \$0.00 | \$5,200.00 | .10 | \$5,200.00 |
| 157 | 1.5.4.2 | Complete Final Design | 1 day | Fr 1/23/18 | Fr 1/23/18 | \$0.00 | \$0.00 | \$2,080.00 | .10 | \$2,288.00 |
| 158 | 1.5.6 | Mechanics Fabrication | 1306 days | Mon 10/3/16 | Fr 10/22/21 | \$0.00 | \$70,000.00 | \$204,840.00 | 0 | \$134,840.00 |
| 159 | 1.5.6.1 | Travel LBNL | 1000 days | Mon 10/3/16 | Thu 8/20/20 | \$0.00 | \$0.00 | \$70,000.00 | 0 | \$0.00 |
| 160 | 1.5.6.2 | Support Structure Cylindrical Structural Shell(CVSS) | 23 days | Wed 11/1/17 | Wed 12/6/17 | \$0.00 | \$0.00 | \$30,761.12 | 0 | \$30,761.12 |
| 161 | 1.5.6.2.1 | Review ALICE CVSS Design | 10 days | Wed 11/1/17 | Wed 11/15/17 | \$0.00 | \$0.00 | \$13,374.40 | .25 | \$13,374.40 |
| 162 | 1.5.6.2.2 | Design-fabrication | 6 days | Thu 11/16/17 | Mon 11/27/17 | \$0.00 | \$0.00 | \$8,024.64 | .25 | \$8,024.64 |
| 163 | 1.5.6.2.3 | CVSS Review Compatibility | 7 days | Tue 11/28/17 | Wed 12/6/17 | \$0.00 | \$0.00 | \$9,362.08 | .25 | \$9,362.08 |
| 164 | 1.5.6.3 | Service Conical Half Shell Review ALICE COSS Design | 15 days | Wed 11/1/17 | Tue 11/22/17 | \$0.00 | \$0.00 | \$26,110.88 | .25 | \$26,110.88 |
| 165 | 1.5.6.3.1 | Service Conical Half Shell Review ALICE COSS Design | 15 days | Wed 11/1/17 | Tue 11/22/17 | \$0.00 | \$0.00 | \$26,061.60 | .25 | \$26,061.60 |

| ID | WBS | Task Name | Duration | Start | Finish | Instantiated | Fixed Cost | Calculate | Cost | Configured | Resource | Cost | Configured |
|-----|------------|--|----------|--------------|--------------|--------------|------------|----------------|----------------|------------|--------------|----------------|------------|
| 170 | 1.5.6.3.2 | Review Design-Fabrication Compatibility | 6 days | Mon 11/27/17 | Mon 12/4/17 | | \$0.00 | \$0.00 | \$8,024.64 | .25 | \$8,024.64 | \$10,030.80 | |
| 171 | 1.5.6.3.3 | COSS Review | 6 days | Tue 12/5/17 | Tue 12/12/17 | | \$0.00 | \$0.00 | \$8,024.64 | .25 | \$8,024.64 | \$10,030.80 | |
| 172 | 1.5.6.4 | Shipping and Storage Containers | 50 days | Tue 8/9/18 | Fri 10/22/18 | | \$0.00 | \$0.00 | \$67,968.00 | .25 | \$67,968.00 | \$84,960.00 | |
| 173 | 1.5.6.4.1 | Design Shipping Cabinets | 39 days | Tue 8/9/18 | Fri 9/24/18 | | \$0.00 | \$0.00 | \$44,928.00 | .25 | \$44,928.00 | \$56,160.00 | |
| 174 | 1.5.6.4.2 | Design Shipping Containers | 20 days | Mon 9/27/18 | Fri 10/22/18 | | \$0.00 | \$0.00 | \$23,040.00 | .25 | \$23,040.00 | \$28,800.00 | |
| 175 | 1.5.7 | Procurements | 650 days | Wed 8/1/18 | Fri 1/29/21 | | \$0.00 | \$2,213,297.00 | \$2,796,969.72 | .25 | \$583,672.72 | \$3,198,600.99 | |
| 176 | 1.5.7.1 | CERN Procurements | 180 days | Fri 11/23/18 | Fri 8/2/19 | | \$0.00 | \$1,026,670.00 | \$1,258,794.80 | .35 | \$207,360.00 | \$1,652,546.50 | |
| 177 | 1.5.7.1.1 | Produce 68 Inner Slaves | 180 days | Fri 11/23/18 | Fri 8/2/19 | | \$0.00 | \$445,670.00 | \$653,030.00 | .35 | \$0.00 | \$881,190.50 | |
| 178 | 1.5.7.1.2 | Slave Production Full Cost Recovery of CERN Manpower | 180 days | Mon 11/26/18 | Fri 8/2/19 | | \$0.00 | \$500,000.00 | \$500,000.00 | .35 | \$0.00 | \$875,000.00 | |
| 179 | 1.5.7.1.3 | Other ITS/CERN Test Equipment Items | 120 days | Mon 11/26/18 | Fri 5/10/19 | | \$0.00 | \$30,000.00 | \$32,764.80 | .25 | \$2,764.80 | \$40,956.00 | |
| 180 | 1.5.7.1.4 | Travel and Per Diem at CERN | 180 days | Mon 11/26/18 | Fri 8/2/19 | | \$0.00 | \$50,000.00 | \$50,000.00 | .10 | \$0.00 | \$55,000.00 | |
| 181 | 1.5.7.2 | Non-CERN Procurements | 180 days | Wed 8/1/18 | Fri 4/12/19 | | \$0.00 | \$1,173,261.00 | \$1,248,940.20 | .25 | \$75,679.20 | \$1,561,175.25 | |
| 182 | 1.5.7.2.1 | Procure 68 Readout RFO Units | 100 days | Mon 11/26/18 | Fri 4/12/19 | | \$0.00 | \$265,740.00 | \$269,740.00 | .25 | \$24,000.00 | \$362,175.00 | |
| 183 | 1.5.7.2.2 | Procure Optical Links 68 | 60 days | Tue 11/27/18 | Mon 2/18/19 | | \$0.00 | \$81,600.00 | \$83,040.00 | .25 | \$1,440.00 | \$103,800.00 | |
| 184 | 1.5.7.2.3 | Procure 100 Cable Reconnects | 100 days | Fri 8/9/18 | Thu 12/20/18 | | \$0.00 | \$161,700.00 | \$164,100.00 | .25 | \$2,400.00 | \$250,125.00 | |
| 185 | 1.5.7.2.4 | PHENIX CRU Production Contingency | 100 days | Fri 8/9/18 | Thu 12/20/18 | | \$0.00 | \$90,000.00 | \$90,000.00 | .25 | \$0.00 | \$112,500.00 | |
| 186 | 1.5.7.2.5 | Procure 100 Samtec Cables | 60 days | Mon 8/6/18 | Fri 10/26/18 | | \$0.00 | \$27,000.00 | \$28,440.00 | .25 | \$1,440.00 | \$35,550.00 | |
| 187 | 1.5.7.2.6 | Fab production PB | 40 days | Thu 8/27/18 | Wed 9/26/18 | | \$0.00 | \$62,973.00 | \$62,973.00 | .25 | \$0.00 | \$78,716.25 | |
| 188 | 1.5.7.2.7 | Procure Power Supplies | 50 days | Fri 8/31/18 | Thu 10/11/18 | | \$0.00 | \$48,015.00 | \$49,167.00 | .25 | \$1,152.00 | \$61,456.75 | |
| 189 | 1.5.7.2.8 | Procure Cooling Plant | 100 days | Mon 8/6/18 | Fri 12/21/18 | | \$0.00 | \$40,000.00 | \$41,440.00 | .25 | \$1,440.00 | \$51,800.00 | |
| 190 | 1.5.7.2.9 | Procure Assembly Fixtures & Jigs | 60 days | Tue 8/7/18 | Mon 10/29/18 | | \$0.00 | \$50,000.00 | \$52,888.00 | .25 | \$2,888.00 | \$65,860.00 | |
| 191 | 1.5.7.2.10 | Procure End Wheels from CERN | 100 days | Wed 8/8/18 | Tue 12/25/18 | | \$0.00 | \$35,548.00 | \$37,863.00 | .25 | \$2,314.00 | \$47,316.25 | |
| 192 | 1.5.7.2.11 | Procure CVSS Material | 5 days | Thu 8/9/18 | Wed 8/15/18 | | \$0.00 | \$30,471.00 | \$42,918.20 | .25 | \$12,447.20 | \$53,847.75 | |
| 193 | 1.5.7.2.12 | Production and test Cylindrical Structural | 70 days | Fri 8/10/18 | Thu 11/15/18 | | \$0.00 | \$4,616.00 | \$4,776.00 | .25 | \$20,160.00 | \$30,970.00 | |
| 194 | 1.5.7.2.13 | Procure COSS Material | 5 days | Mon 8/13/18 | Fri 8/17/18 | | \$0.00 | \$50,000.00 | \$50,000.00 | .25 | \$0.00 | \$62,500.00 | |
| 195 | 1.5.7.2.14 | Procure Shipping and Storage Containers | 60 days | Wed 8/17/18 | Tue 10/23/18 | | \$0.00 | \$0.00 | \$0.00 | .25 | \$0.00 | \$0.00 | |
| 196 | 1.5.7.2.15 | Procure Detector Half Brackets | 100 days | Mon 8/13/18 | Fri 12/28/18 | | \$0.00 | \$13,000.00 | \$14,552.00 | .25 | \$1,552.00 | \$18,190.00 | |
| 197 | 1.5.7.2.16 | Procure Service Half Brackets | 100 days | Tue 8/14/18 | Mon 12/31/18 | | \$0.00 | \$120,000.00 | \$121,552.00 | .25 | \$1,552.00 | \$151,940.00 | |
| 198 | 1.5.7.2.17 | Procure Detector and Service Half Brackets | 100 days | Wed 8/15/18 | Wed 11/1/19 | | \$0.00 | \$21,000.00 | \$22,552.00 | .25 | \$1,552.00 | \$28,190.00 | |
| 199 | 1.5.7.2.18 | Procure Halo Halls Super Slits | 100 days | Thu 8/16/18 | Wed 11/21/19 | | \$0.00 | \$51,597.00 | \$53,149.00 | .25 | \$1,552.00 | \$66,456.25 | |
| 200 | 1.5.7.3 | Assembly and Testing | 610 days | Thu 9/27/18 | Fri 1/29/21 | | \$0.00 | \$14,366.00 | \$312,234.72 | .25 | \$297,868.72 | \$384,879.24 | |
| 201 | 1.5.7.3.1 | Test Power PB | 10 days | Thu 9/27/18 | Wed 10/10/18 | | \$0.00 | \$0.00 | \$11,620.00 | .25 | \$11,620.00 | \$1,440.00 | |
| 202 | 1.5.7.3.2 | Ship PB to BNL | 5 days | Thu 10/11/18 | Wed 10/17/18 | | \$0.00 | \$0.00 | \$11,520.00 | .25 | \$11,520.00 | \$1,440.00 | |
| 203 | 1.5.7.3.3 | Test Power Supplies at BNL | 10 days | Fri 10/12/18 | Thu 10/25/18 | | \$0.00 | \$0.00 | \$11,520.00 | .25 | \$11,520.00 | \$1,440.00 | |
| 204 | 1.5.7.3.4 | Test Production FENS e-Links, CRU, optical System | 60 days | Mon 4/15/19 | Fri 7/5/19 | | \$0.00 | \$0.00 | \$21,600.00 | .25 | \$2,160.00 | \$27,000.00 | |
| 205 | 1.5.7.3.5 | Assembly & Test Cooling | 20 days | Mon 12/24/18 | Fri 1/18/19 | | \$0.00 | \$0.00 | \$14,400.00 | .25 | \$14,400.00 | \$18,000.00 | |
| 206 | 1.5.7.3.6 | Slave Receipt Inspection | 10 days | Mon 8/6/19 | Fri 8/16/19 | | \$0.00 | \$0.00 | \$5,760.00 | .25 | \$5,760.00 | \$7,200.00 | |

| ID | WBS | Task Name | Duration | Start | Finish | Install/Fixed Cost | Calculate fixed cost | Cost | contingent/Resource Cost | cost+contingent | |
|-----|-------------|---|----------|--------------|-------------------|--------------------|----------------------|-------------|--------------------------|-----------------|--------------|
| 207 | 1.5.7.3.7 | Individual Slave test and rework | 70 days | Mon 8/19/19 | Fri 11/22/19 LBNL | \$0.00 | \$0.00 | \$16,128.00 | .25 | \$16,128.00 | \$20,160.00 |
| 208 | 1.5.7.3.8 | Layer Assembly and Test | 105 days | Mon 11/25/19 | Fri 4/17/20 LBNL | \$0.00 | \$5,355.00 | \$67,537.64 | .25 | \$62,182.64 | \$84,422.05 |
| 209 | 1.5.7.3.8.1 | Test Installation of Slaves onto End | 20 days | Mon 11/25/19 | Fri 12/20/19 | \$0.00 | \$0.00 | \$7,282.88 | .25 | \$7,282.88 | \$9,103.60 |
| 210 | 1.5.7.3.8.2 | Half-Detector Assembly Review | 5 days | Mon 12/23/19 | Fri 12/27/19 LBNL | \$0.00 | \$0.00 | \$2,674.88 | .25 | \$2,674.88 | \$3,343.60 |
| 211 | 1.5.7.3.8.3 | Install Slaves onto End Wheels | 3.5 days | Mon 12/30/19 | Fri 2/14/20 LBNL | \$2,770.00 | \$2,770.00 | \$24,228.08 | .25 | \$21,458.00 | \$30,285.10 |
| 212 | 1.5.7.3.8.4 | Test and Rework Layers after Assembly | 30 days | Mon 2/17/20 | Fri 3/27/20 LBNL | \$2,585.00 | \$2,585.00 | \$16,071.80 | .25 | \$13,486.80 | \$20,089.75 |
| 213 | 1.5.7.3.8.5 | Perform Half Detector Metrology | 15 days | Mon 3/30/20 | Fri 4/17/20 LBNL | \$0.00 | \$0.00 | \$17,280.00 | .25 | \$17,280.00 | \$21,600.00 |
| 214 | 1.5.7.3.8.6 | Milestone Complete | 0 days | Fri 4/17/20 | Fri 4/17/20 LBNL | \$0.00 | \$0.00 | \$0.00 | .25 | \$0.00 | \$0.00 |
| 215 | 1.5.7.3.9 | Barrel Assembly and Test | 85 days | Mon 4/20/20 | Fri 6/14/20 LBNL | \$0.00 | \$9,011.00 | \$87,948.44 | .25 | \$78,937.44 | \$109,610.55 |
| 216 | 1.5.7.3.9.1 | Assemble Layers and CYS into Half Detector | 40 days | Mon 4/20/20 | Fri 6/12/20 LBNL | \$0.00 | \$0.00 | \$46,372.16 | .25 | \$46,372.16 | \$57,665.20 |
| 217 | 1.5.7.3.9.2 | Test and Rework Half Detector | 10 days | Mon 6/15/20 | Fri 6/26/20 LBNL | \$2,585.00 | \$2,585.00 | \$7,934.76 | .25 | \$5,349.76 | \$9,918.45 |
| 218 | 1.5.7.3.9.3 | Perform Half Detector Metrology on Final Assembly | 10 days | Mon 6/29/20 | Fri 7/10/20 LBNL | \$0.00 | \$0.00 | \$11,520.00 | .25 | \$11,520.00 | \$14,400.00 |
| 219 | 1.5.7.3.9.4 | Validation of Final Assembly | 15 days | Mon 7/13/20 | Fri 7/31/20 LBNL | \$2,585.00 | \$2,585.00 | \$13,201.64 | .25 | \$10,616.64 | \$16,502.05 |
| 220 | 1.5.7.3.9.5 | Packaging Final Assemblies to BNL | 10 days | Mon 8/3/20 | Fri 8/14/20 LBNL | \$3,841.00 | \$3,841.00 | \$8,819.88 | .25 | \$4,978.88 | \$11,024.85 |
| 221 | 1.5.7.3.10 | Metrology on Slave Assemblies | 30 days | Mon 8/17/20 | Fri 9/25/20 LBNL | \$0.00 | \$0.00 | \$17,880.00 | .25 | \$17,880.00 | \$22,350.00 |
| 222 | 1.5.7.3.11 | Assemble full ladders into Half support | 50 days | Mon 9/28/20 | Fri 12/4/20 LBNL | \$0.00 | \$0.00 | \$24,832.00 | .25 | \$24,832.00 | \$31,040.00 |
| 223 | 1.5.7.3.12 | Metrology on Final Assembly | 10 days | Mon 12/7/20 | Fri 12/18/20 LBNL | \$0.00 | \$0.00 | \$10,400.00 | .25 | \$10,400.00 | \$13,000.00 |
| 224 | 1.5.7.3.13 | Half detector Assembly Readout and Coating | 30 days | Mon 12/21/20 | Fri 1/29/21 | \$0.00 | \$0.00 | \$21,656.64 | 0 | \$21,656.64 | \$21,656.64 |
| 225 | 1.5.8 | Installation | 131 days | Mon 2/11/21 | Mon 8/2/21 | \$0.00 | \$0.00 | \$45,248.00 | .25 | \$45,248.00 | \$63,160.00 |
| 226 | 1.5.8.1 | Installation Prop | 10 days | Mon 2/15/21 | Fri 2/19/21 LBNL | \$0.00 | \$0.00 | \$15,520.00 | .10 | \$15,520.00 | \$19,400.00 |
| 227 | 1.5.8.2 | Installation Review | 1 day | Mon 2/15/21 | Mon 2/15/21 LBNL | \$0.00 | \$0.00 | \$2,080.00 | .10 | \$2,080.00 | \$2,288.00 |
| 228 | 1.5.8.3 | Installation | 30 days | Tue 2/16/21 | Mon 3/29/21 LBNL | \$0.00 | \$0.00 | \$27,648.00 | .50 | \$27,648.00 | \$41,472.00 |
| 229 | 1.5.8.4 | Commissioning | 90 days | Tue 3/30/21 | Mon 6/21/21 | \$0.00 | \$0.00 | \$0.00 | 0 | \$0.00 | \$0.00 |
| 230 | 1.5.9 | Ready for beam | 0 days | Mon 6/22/21 | Mon 6/22/21 | \$0.00 | \$0.00 | \$0.00 | 0 | \$0.00 | \$0.00 |



734 **10 Abbreviations and Code Names**

| | | |
|-----|------|--|
| | MAPS | Monolithic Active Pixel Sensors |
| | MVTX | MAPS-based Vertex Detector |
| | QGP | Quark Gluon Plasma |
| 735 | DCA | Distance of Closest Approach |
| | RHIC | Relativistic Heavy Ion Collider at BNL |
| 736 | LHC | Large Hadron Collider at CERN |

11 Literature Cited

References

- [1] A. Adare et al. Energy Loss and Flow of Heavy Quarks in Au+Au Collisions at $\sqrt{s_{NN}} = 200$ GeV. *Phys. Rev. Lett.*, 98:172301, 2007.
- [2] B.I. Abelev et al. Transverse Momentum and Centrality Dependence of High- p_T Nonphotonic Electron Suppression in Au+Au Collisions at $\sqrt{s_{NN}} = 200$ GeV. *Phys. Rev. Lett.*, 98:192301, 2007.
- [3] L. Adamczyk et al. Observation of D^0 Meson Nuclear Modifications in Au+Au Collisions at $\sqrt{s_{NN}} = 200$ GeV. *Phys. Rev. Lett.*, 113(14):142301, 2014.
- [4] Betty Abelev et al. Suppression of high transverse momentum D mesons in central Pb-Pb collisions at $\sqrt{s_{NN}} = 2.76$ TeV. *JHEP*, 09:112, 2012.
- [5] J.C. Xu, J.F. Liao, and M. Gyulassy. Bridging soft-hard transport properties of quark-gluon plasmas with cujet3.0. *JHEP*, 1602:169, 2016.
- [6] L. Adamczyk et al. Measurement of D^0 azimuthal anisotropy at mid-rapidity in Au+Au collisions at $\sqrt{s_{NN}} = 200$ GeV. 2017.
- [7] S.K. Das, F. Scardina, S. Plumari, and V. Greco. Heavy-flavor in-medium momentum evolution: Langevin versus boltzmann approach. *Phys. Rev.*, C90:044901, 2014.
- [8] Serguei Chatrchyan et al. Evidence of b-Jet Quenching in PbPb Collisions at $\sqrt{s_{NN}} = 2.76$ TeV. *Phys. Rev. Lett.*, 113(13):132301, 2014. [Erratum: *Phys. Rev. Lett.* 115,no.2,029903(2015)].
- [9] Jinrui Huang, Zhong-Bo Kang, and Ivan Vitev. Inclusive b-jet production in heavy ion collisions at the LHC. *Phys. Lett.*, B726:251–256, 2013.
- [10] sPHENIX preConceptual Design Report. 2015.
- [11] A. Adare et al. An Upgrade Proposal from the PHENIX Collaboration. 2015.
- [12] B Abelev et al. Technical Design Report for the Upgrade of the ALICE Inner Tracking System. *J. Phys.*, G41:087002, 2014.
- [13] Gianluca Aglieri Rinella. The ALPIDE pixel sensor chip for the upgrade of the ALICE Inner Tracking System. *Nucl. Instrum. Methods Phys. Res., A*, xx:xx, 2016. In Press.
- [14] M. Mager. ALPIDE, the Monolithic Active Pixel Sensor for the ALICE ITS upgrade. *Nucl. Instrum. Meth.*, A824:434–438, 2016.
- [15] CMS Collaboration. Transverse momentum balance of b-jet pairs in PbPb collisions at 5 TeV. 2016.
- [16] E. Norrbin and T. Sjostrand. Production and hadronization of heavy quarks. *Eur. Phys. J.*, C17:137–161, 2000.
- [17] Jinrui Huang, Zhong-Bo Kang, Ivan Vitev, and Hongxi Xing. Photon-tagged and B-meson-tagged b-jet production at the LHC. *Phys. Lett.*, B750:287–293, 2015.
- [18] CMS Collaboration. Splitting function in pp and PbPb collisions at 5.02 TeV. 2016.

- 771 [19] K Kauder. Measurement of the Shared Momentum Fraction z_g using Jet Reconstruction in p+p and
772 Au+Au Collisions with STAR. 2016.
- 773 [20] Andrew J. Larkoski, Simone Marzani, Gregory Soyez, and Jesse Thaler. Soft Drop. *JHEP*, 05:146,
774 2014.
- 775 [21] S. S. Cao, G.Y. Qin, and S. A. Bass. Energy loss, hadronization and hadronic interactions of heavy
776 flavors in relativistic heavy-ion collisions. *Phys. Rev.*, C92:024907, 2015.
- 777 [22] Min He, Rainer J. Fries, and Ralf Rapp. Heavy-Quark Diffusion and Hadronization in Quark-Gluon
778 Plasma. *Phys. Rev.*, C86:014903, 2012.
- 779 [23] J. Anderson et al. FELIX: a PCIe based high-throughput approach for interfacing front-end and trigger
780 electronics in the ATLAS Upgrade framework. *JINST*, 11(12):C12023, 2016.
- 781 [24] S. Adler et al. Phenix on-line systems. *Nucl. Instrum. Meth. A*, 499:560, 2003.
- 782 [25] S. Agostinelli et al. GEANT4: A Simulation toolkit. *Nucl. Instrum. Meth.*, A506:250–303, 2003.
- 783 [26] Johannes Rauch and Tobias Schlter. GENFIT a Generic Track-Fitting Toolkit. *J. Phys. Conf. Ser.*,
784 608(1):012042, 2015.
- 785 [27] Wolfgang Waltenberger. RAVE: A detector-independent toolkit to reconstruct vertices. *IEEE Trans.*
786 *Nucl. Sci.*, 58:434–444, 2011.